

Real-Time Loss Tools: Open-Source Software for Time- and State-Dependent Seismic Damage and Loss Calculations – Features and Application to the 2023 Türkiye-Syria Sequence

C.I. Nieves  *¹, H. Crowley  ^{2,3}, G. Weatherill  ¹, F. Cotton  ^{1,4}

¹Seismic Hazard and Risk Dynamics, GFZ Helmholtz Centre for Geosciences, Potsdam, Germany, ²Global Earthquake Model (GEM) Foundation, Pavia, Italy, ³EUCENTRE, Pavia, Italy (formerly), ⁴Institute of Geosciences, University of Potsdam, Potsdam, Germany

Author contributions: *Conceptualization:* C.I. Nieves, H. Crowley, G. Weatherill. *Methodology:* C.I. Nieves, H. Crowley, G. Weatherill. *Software:* C.I. Nieves, G. Weatherill. *Validation:* C.I. Nieves, G. Weatherill. *Writing - Original draft:* C.I. Nieves, H. Crowley, G. Weatherill. *Writing - Review & Editing:* C.I. Nieves, H. Crowley, G. Weatherill, F. Cotton.

Abstract During a seismic sequence, each earthquake has the potential to damage and weaken exposed structures, causing their fragility to change, and increasing their likelihood of being further damaged by subsequent earthquakes. At the same time, building occupants that need to be hospitalised will not be present in the buildings whose damage led to their hospitalisation during any subsequent events, for as long as they remain in hospital. These changes in the fragility of buildings and the location of building occupants have an impact on the estimation of damage and losses throughout a seismic sequence, but are rarely accounted for in calculations. Building upon OpenQuake, we have developed the Real-Time Loss Tools software to address the lack of a publicly available open-source software able to account for these factors. We present its main features, together with a case-study focused on the 2023 Türkiye-Syria earthquakes. This application shows the relevance of accounting for damage accumulation and the relocation of people, particularly when large ruptures affect a vast area. Comparisons of economic losses calculated with and without damage accumulation show a larger discrepancy at the local level (up to 50%, depending on the method) than when aggregating results by province (up to 14%).

Non-technical summary It is common for earthquakes not to occur in an isolated fashion but as part of a sequence comprising often a large mainshock and a series of smaller aftershocks, or a cluster of similarly-sized events. Some buildings might only suffer from slight or moderate damage due to one earthquake, but this damage reduces their capability to withstand further earthquakes that happen in a period of time shorter than that needed to repair or strengthen them before the next one hits. Similarly, people might not be able to return to buildings either due to their own death or hospitalisation, or because it takes time to inspect and repair building damage. It is only in recent years that models and tools have started to be developed to be able to take these factors into account when carrying out computer-based estimates of damage, injuries and deaths due to a series of earthquakes but, so far, there has been no publicly available open-source software able to do this. This was the main motivation for building upon the well-established OpenQuake software and developing the Real-Time Loss Tools, which are presented in this paper together with an illustrative application focused on the 2023 Türkiye-Syria earthquakes.

1 Introduction

The occurrence of an earthquake with the potential to cause damage and losses invariably prompts questions as to what to expect in the immediate future, in the form of both direct consequences of the event itself, as well as subsequent seismic activity. These questions may arise from a variety of stakeholders, including governments, first responders, civil protection bodies, international aid organisations, insurance companies, the me-

dia and the general public. As a first step, there is an urgent need to understand, at least in qualitative terms, whether the earthquake is expected to result in major, minor or no impact, by means of a so-called *Rapid Impact Assessment* (e.g., Earle et al., 2009; Lilienkamp et al., 2023). A quantitative estimate of losses, in terms of number of damaged or collapsed buildings, number of injuries, fatalities and displaced people, as well as direct economic losses, becomes relevant as a second step (e.g., within the first half hour after the earthquake), and constitutes what is usually referred to as *Rapid Loss Assessment* (RLA). RLA results can be used, for example, by first responders and civil protection agencies to send

Production Editor:
Théa Ragon
Handling Editor:
Vitor Silva
Copy & Layout Editor:
Anna Ledeczi

Received:
20 February 2024
Accepted:
3 February 2025
Published:
1 April 2025

*Corresponding author: cecilia.nieves@gfz.de

the right teams and equipment to search for trapped survivors and prepare emergency shelter, by governments to allocate funding and request international aid, or by insurance companies to plan post-earthquake assessments of damage to manage potential claims.

Rapid estimates of damage become more challenging, however, when strong aftershocks (or, more generally, subsequent earthquakes in the sequence) hit in quick succession and the economic and human consequences stem no longer from one event but from a series of events. It is known that previously-damaged buildings are more vulnerable when subject to a subsequent shock due to damage accumulation (Yeo and Cornell, 2005; Mouyiannou et al., 2014; Bazzurro et al., 2004; Polese et al., 2013), as has been demonstrated in the 2010/2011 Christchurch (New Zealand) (Moon et al., 2014), 2012 Emilia Romagna (Italy) (Sorrentino et al., 2013), and the 2016/2017 Central Italy (Rossi et al., 2019) earthquakes. Moreover, the location of people becomes even more uncertain than usual in the immediate aftermath of an event, as injured people may be taken to hospital, some people may remain trapped, some others may have already been placed in shelters or may simply decide to stay outside, increasing the uncertainty in the estimation of further casualties. The matter of damage accumulation can be tackled by means of so-called *state-dependent* fragility models that indicate the probability of exceeding a series of damage states as a function of not only the intensity of ground shaking but also the current damage state of the structure. Efforts continue to be dedicated to the derivation of such models (e.g., Iacchetti et al., 2023; Orlicchio, 2022). Due to its complexity, the modelling of the movement of people has so far received less attention and existing methods and software focus on the estimation of numbers of displaced people and the need for short-term shelter (e.g. HAZUS-MH (Federal Emergency Management Agency, 2003), MCEER (Chang et al., 2008)), the demands on the health system and potential transfer of patients between different hospitals (e.g., Ceferino et al., 2020), and/or longer-term returns/relocations (Costa et al., 2022) after a major earthquake, not on the effects of people relocation on the calculation of injuries and deaths during a seismic sequence.

Complementary to the capacity to quickly estimate losses that have already occurred is the possibility of forecasting the evolution of seismicity and potential further losses in the short-term (hours, weeks, months), particularly after the occurrence of an event of large magnitude that will most likely be followed by aftershocks. Although short-term seismicity forecasts have been available for several years, *Operational Earthquake Forecasting* (OEF) systems that implement them are currently running only in a small number of countries, including Italy, New Zealand and the United States (Marzocchi et al., 2014; Gerstenberger et al., 2014; Michael et al., 2019). Such systems usually report on probabilities or expected number of earthquakes above a certain magnitude in the next many days of interest (e.g. 1 day, 1 week), considering not only the baseline “normal” seismicity but, most importantly, the history of seismicity until the point in time in which the calcu-

lation is run. The capability of estimating losses due to these forecasts, so-called *Operational Earthquake Loss Forecasting* (OELF), has so far only been implemented in Italy by means of the MANTIS-K system (Iervolino et al., 2015), and only been recently expanded into MANTIS v2.0 to account for damage accumulation by means of state-dependent fragility models (Chioccarelli et al., 2022). The exact application of OEF and OELF within decision-making frameworks is still a matter of debate (e.g., Woo and Marzocchi, 2014), but they are expected to facilitate the implementation of risk-mitigation measures in near-real time.

While existing research has addressed several components of the estimation of damage and losses during seismic sequences (e.g., Papadopoulos and Bazzurro, 2020; Trevisopoulou et al., 2020; Iacchetti et al., 2024), there had been so far no publicly available open-source software that was able to carry out damage and loss calculations of earthquake sequences/seismicity forecasts accounting for damage accumulation and the displacement of the building occupants along the process, as well as external sources of damage estimation. This was a large motivation for the development of the *Real-Time Loss Tools* (RTLs) software presented herein (Nievas et al., 2023c). The software was born within the framework of the European Horizon 2020 RISE project¹, with the initial objective of demonstrating how the different components of real-time damage and loss calculations for earthquake sequences could be integrated. As work progressed, the need emerged for a transparent and publicly-available software that the research community could use as a starting point to explore the different aspects of this integration and develop strategies and research questions for potential future scalability and operationalisation. Because the use and promotion of open-source software lies at the heart of transparency, the *Real-Time Loss Tools* are coded in Python 3, rely on the well-established, open-source OpenQuake engine (Pagani et al., 2014; Silva et al., 2013) to estimate ground motions and calculate damage, and are released under the GNU AGPL v3.0 license. Within the large scope of post-earthquake consequences that can be of interest for a seismic loss assessment, which include, among others, damage to lifelines, damage/interruption of roads/transportation, need for hospital beds, and costs of business down-time, the RTLs currently focus on damage to buildings and estimation of human casualties as main outputs.

This paper presents the *Real-Time Loss Tools*, its algorithms and rationale, as well as an example application to the February 2023 Türkiye/Syria earthquakes, which featured moment magnitude M_w 7.8 and M_w 7.5 earthquakes within the space of nine hours, followed by an aftershock sequence lasting several months and producing further two earthquakes with M_w 6+ and 19 with M_w 5+. Section 2 presents an overview of the software and its main features, while section 3 goes into the detail of the calculation workflows. The example application and its results are presented in section 4. We show that, due to the large spatial extent of the shaking, there

¹<http://rise-eu.org/home/>

are areas expected to have been mostly affected by only one of the two $M_w 7+$ earthquakes, and areas expected to have experienced relevant shaking and damage from both, and that these spatial differences have a relevant impact on the losses calculated accounting or not for damage accumulation. Further details on the software and different case-study applications for both RLA and OELF can as well be found in [Nievas et al. \(2023a,d\)](#).

2 Software overview

The *Real-Time Loss Tools* (RTLs) are a software that calculates numbers of damaged buildings, economic losses and human casualties due to the occurrence of several earthquakes during a short time span, accounting for the accumulation of damage as well as the relocation of building occupants during the seismic sequence and at different times of the day. Ground shaking and damage are calculated by the OpenQuake engine ([Paganì et al., 2014](#); [Silva et al., 2013](#)), which is called internally by the RTLs for this purpose, while losses and casualties are handled separately by the RTLs themselves. They feature two main algorithms, one focused on RLA and the other on OELF, which can be executed as a series in a chronological order specified by the user. The OELF routine is event-based, following the recent shift in the OEF community from models that output gridded seismicity rates for a time span of interest to models that generate a large number of stochastic earthquake catalogues for that same time span (e.g., [Savran et al., 2020](#)). Each of these stochastic catalogues is a possible realisation of seismicity for that period of time.

Both RLA and OELF algorithms of the RTLs calculate cumulative damage, losses and casualties due to sequences of fictitious or real earthquakes, but they differ in their assumptions and some of their internal workings:

- A RLA calculation expects detailed information about the specific earthquake rupture (in the form of an OpenQuake rupture file or by specifying the fault geometry, strike, dip, and rake, in addition to magnitude and hypocentral location), and it updates what the software considers to be the current exposure model, which will be used in subsequent RLA and OELF calculations. Each RLA calculation deals with one input earthquake. A sequence of earthquakes is calculated when a series of RLA triggers are input by the user.
- An OELF calculation assumes there will be several earthquakes listed in its catalogue input file. The listed earthquakes may all belong to the same sequence or different sequences. Within the context of earthquake forecasting, each sequence would correspond to a possible realisation of seismicity (or stochastic event set, SES, following the nomenclature used by OpenQuake). When the input catalogue contains several SES (to account for epistemic uncertainty), each catalogue is processed independently and their damage and loss results are

averaged at the end. The OELF calculation does not take specific rupture details but calculates them in a stochastic fashion using a uniform-area seismic source model in the OpenQuake format, provided as input by the user. Earthquakes listed for an OELF calculation can be minimally characterised by their epicentral coordinates, magnitude and UTC date/time.

From the descriptions above it becomes apparent that the concepts of RLA and OELF are used to name and explain the algorithms in the RTLs due to the simplicity with which they convey the kind of calculation that is being carried out. However, as the user is free to run the calculations for any (set of) earthquake(s) at any time, it is clear that the RTLs are not running RLA and OELF calculations strictly speaking (i.e., triggered by the occurrence of an earthquake in real life) but the fundamental calculations that would allow RLAs and/or OELFs to be carried out in real time if desired. Moreover, the application of the two workflows is not limited to RLA and OELF. For example, the RLA workflow is useful not only for real earthquake sequences but also for what-if cascade scenarios that may be relevant for emergency planning by civil protection agencies, while the OELF workflow may also be relevant for longer-term time-dependent probabilistic risk assessments as well as what-if induced-seismicity applications, using catalogues generated by geomechanical models/simulations as input.

As shown in the general overview depicted in [Figure 1](#), many inputs needed to run the RTLs correspond to those needed to run a scenario damage or loss calculation in OpenQuake², with some additions, and many of the inputs are common to both the RLA and OELF algorithms. Some of the inputs remain the same during the calculation, while others, such as the OpenQuake configuration file and the exposure model, are updated by the RTLs. All inputs are user-defined. The standard working of the software expects the user to input state-dependent fragility models, but allows for the possibility of using state-independent fragilities as well, making it possible to at least partly account for exposure dynamics when state-dependent fragility models are not yet available for the case-study under consideration (this approach is described in [8](#)). The RTLs allow the user to provide an external estimation of damage for individual buildings, if desired. For example, this can come from structural health monitoring (SHM) techniques or direct observations in the field.

The final outputs focus on results on damage, economic losses and human casualties, the latter according to a user-defined injury scale. The intermediate outputs generated by the RTLs can be of interest themselves, as they provide snapshots of the status of the exposed buildings (including their state of damage, which further informs their level of vulnerability) and people after each individual earthquake in the form of updated exposure models, timelines of building usability and hospitalisations/deaths. At locations where the exposure model contains aggregated numbers of buildings,

²<https://docs.openquake.org/oq-engine/master/manual/>

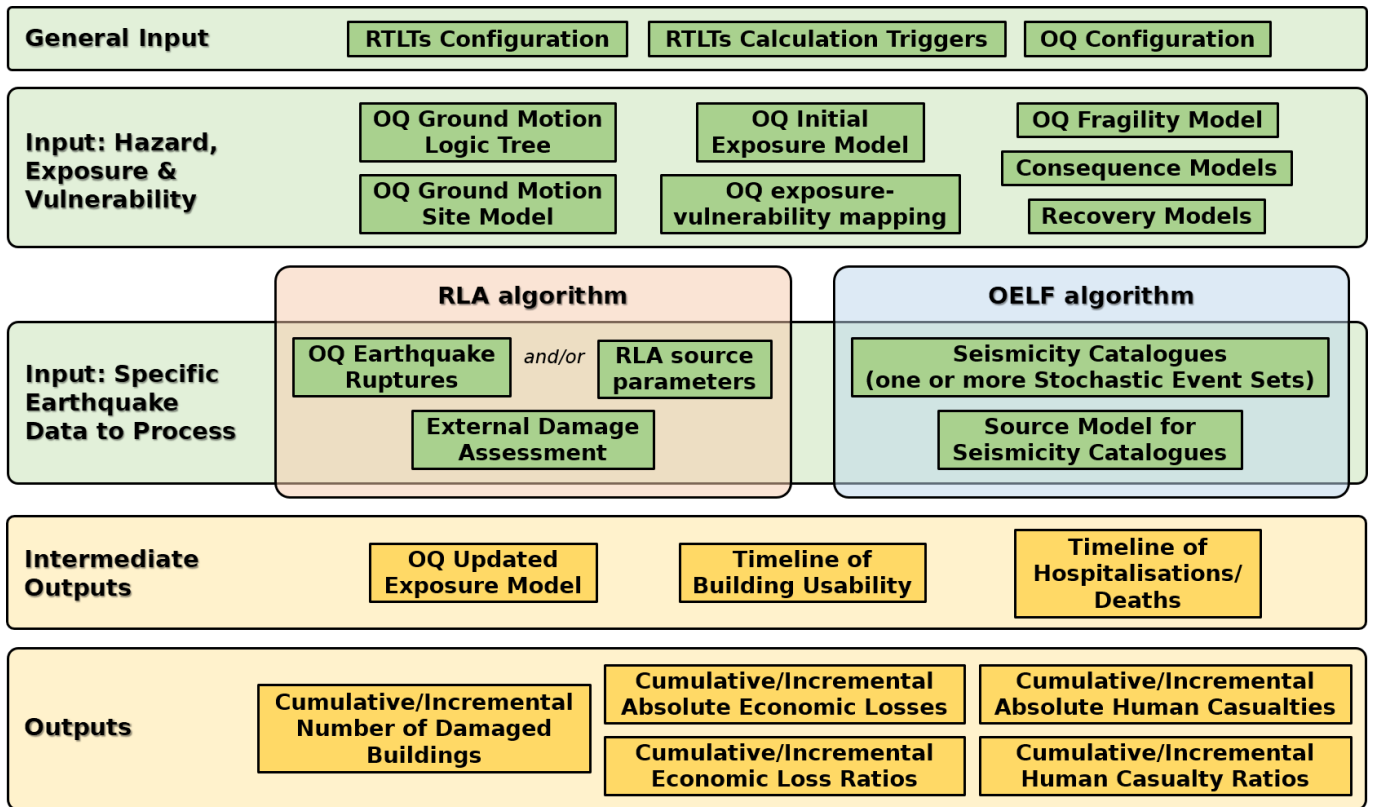


Figure 1 General overview of the inputs (green) and outputs (yellow) of the Real Time Loss Tools. Inputs labelled “OQ” are directly used by OpenQuake, while the rest are used by the RTLs.

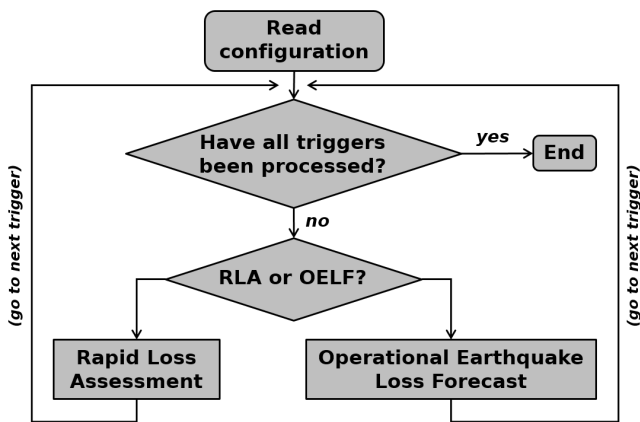


Figure 2 General overview of the main algorithm of the Real Time Loss Tools.

the RTLs output numbers of buildings in each damage state, while the output refers to probabilities of a building resulting in each damage state where the exposure model refers to individual buildings. A combination of both types of exposure is possible.

A series of configuration parameters and a list of calculation triggers are needed to run the software. The latter indicate whether a RLA or an OELF are to be run, the order in which they are to be run, and the names of the files with the associated earthquake parameters or catalogues. The RTLs process each trigger at a time, accessing the RLA or OELF routine as indicated (Figure 2). The OpenQuake engine (Pagani et al., 2014; Silva et al., 2013) is called from within the routines to estimate ground motions and damage states. In the case of a RLA this oc-

curs just once, while in the case of OELF this occurs for each earthquake in the seismicity forecast, controlled by two loops: a main one that loops through each SES and a second one that loops through each earthquake within the SES. External sources of damage estimates, if provided as input by the user, are retrieved and used for RLAs but not OELFs (as OELFs forecast damage yet to occur), though they do influence the damage and losses from OELF (in the form of pre-existing damage in the exposure model) if provided for RLA in a calculation that contains both RLA and OELF triggers. OpenQuake input files are updated for each earthquake run.

Apart from the specific damage and loss outputs up to that point in time, each RLA results in two kinds of output that have an influence on the subsequent calculations: (1) an update of the exposure model files to reflect the current expectation of damage of the building stock, and (2) future timelines of building usability and hospitalisations/deaths, based on the damage and injuries/deaths up to that point in time (see Figure 1). These files are then used by all RLAs and OELFs that follow, as illustrated in Figure 3, as they allow for the accumulation of damage and the variation in the number of occupants of buildings along the sequence. OELF calculations do produce similar outputs but they are used only for the subsequent earthquakes within the same stochastic event set, as OELFs are estimates of the future that may or may not occur; the current expectation of damage stemming from earthquakes that have actually happened (calculated in all previous RLAs) is read at the beginning of each stochastic event set. Although the example in Figure 3 focuses on a series of alternate RLA

and OELF calculations, the RTLs can take any user-defined series of triggers (all RLAs, all OELFs, any mix of the two). Analogous diagrams could be drawn for the future timelines of building usability and hospitalisations/deaths, the only difference being that these timelines are read by all subsequent earthquakes (to consider, for example, all people who are still away due to all previous earthquakes) and not just the first subsequent one; the distinction between the RLA and OELF cases remains the same.

The number of occupants in the buildings is determined just before running the RLA or a specific earthquake of the OELF, considering appropriate factors for the time of the day at which the current earthquake occurs (in local time) and the expected casualties from earthquakes run up to that point in time (all RLAs and, if within an OELF calculation, all previous earthquakes within the same SES). This requires that all earthquake catalogues both for RLA and OELF contain date and time of occurrence.

As the RTLs make use of the OpenQuake engine (Pagani et al., 2014; Silva et al., 2013) for calculating ground motions and damage, they naturally inherit features and capabilities of OpenQuake even if they are not described herein or in the RTLs' documentation, as long as the additional specific configuration parameters and input files do not need updating for different earthquakes in the sequence. Being open-source, the possibility of incorporating OpenQuake features not considered herein (or developed in the future) is always open, as the code of the RTLs can be modified to satisfy the need for additional input.

3 Calculation workflows

3.1 Rapid Loss Assessment

A standard RLA run in the OpenQuake engine starts with the calculation of a number of ground motion fields associated with different branches of the ground motion logic tree as well as different stochastic realisations of the epistemic and aleatory uncertainties inherent of the selected ground motion models. The expected number of damaged buildings, economic losses and human casualties are calculated for each ground motion field by means of fragility and vulnerability models, and combined together as per the weights of the branches of the logic tree. When the vulnerability models include a characterisation of their uncertainty, OpenQuake (though not yet the RTLs) generates random samples of loss ratios for each ground motion field at each location.

To this general flow, the RTLs add the updating of the exposure model to reflect the current expected damage state of the buildings after each earthquake, the calculation of timelines of building usability and hospitalisations/deaths, as well as the retrieval of the latter for the purpose of updating the number of building occupants at the time of the subsequent earthquake in the sequence (Figure 4).

Because in a real-time application the time of occurrence of earthquake $i+1$ is unknown at the time of oc-

currence of earthquake i , the RLA routine begins with the examination of the local time of the earthquake and its translation into one of the three possible times of the day defined in the European Seismic Risk Model 2020 (ESRM20 Crowley et al., 2021), which are modified from the PAGER population distribution model (Jaiswal and Wald, 2010): day (10 am to 6 pm), night (10 pm to 6 am) and transit (6 am to 10 am, and 6 pm to 10 pm). This classification is used to calculate the number of occupants in each building, which is based on the number of census occupants in the exposure model and a series of factors (used to multiply the census occupants) defined in the configuration file for the three possible times of the day and each occupancy case that exists in the exposure model (e.g., residential, commercial, industrial). The word "census" is used in the RTLs to refer to the number of occupants assigned to a building irrespective of the time of the day, even if this number has not been obtained from census data. The RTLs makes no assumptions regarding the magnitude of the time-of-day factors specified and the user has complete freedom to decide whether to use factors smaller than 1, which will lead to the number of occupants considered being smaller than the census occupants, or larger than 1 for the opposite effect.

The updating of building occupants requires not only that the local time of occurrence be known but also that the RTLs retrieve information on injured, deceased and displaced people due to earthquakes for which RLAs have already been run. The RLA function calls a routine that is able to retrieve this information from previously-stored files and combine it with the number of census occupants and the time of the day factors, to finally produce an updated number of occupants at the time of the earthquake being run. The details on this calculation are provided under 3.4.

After updating a series of OpenQuake input files, the OpenQuake engine is called to calculate ground motions and damage estimates using its scenario damage calculator. These results, which are based fully on ground motion, exposure and vulnerability models, may also be enriched in the RTLs through other sources of damage information, such as direct field inspections or the continuous monitoring of structures by means of permanently-installed sensors, which opens the possibility of estimating probabilities of damage based on parameters calculated from the waveforms recorded at various positions throughout the buildings (SHM). Recent research has been dedicated to identifying the most suitable parameters for such a purpose (e.g., Reuland et al., 2023) and developing strategies to distinguish changes in the dynamic properties of structures driven by damage from their natural fluctuations (e.g., Guéguen and Tiganescu, 2018) or accounting for material recovery (e.g. Astorga and Guéguen, 2020).

Once the damage results are retrieved from OpenQuake, the RTLs pass on these results and the user-input-defined external damage probabilities to the routine that updates and stores the exposure model to reflect the current expectation of damage (further details under 3.3). External damage probabilities need to be specified by the user using the same damage scale as

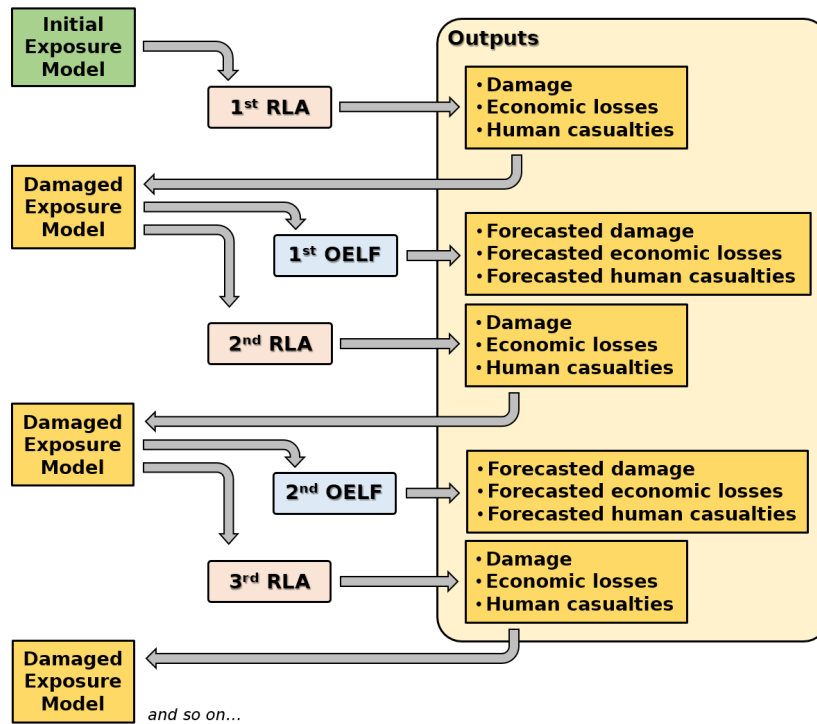


Figure 3 Schematic representation of the interaction between the RLA and OELF algorithms around the updating of the damaged exposure model.

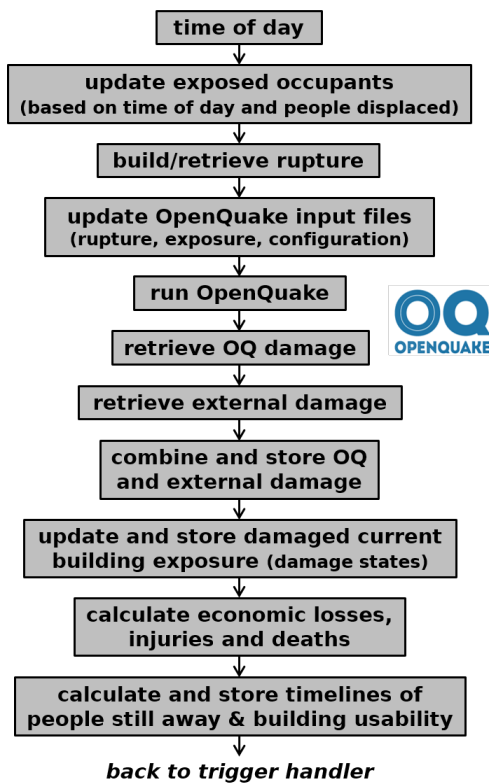


Figure 4 Main tasks of the RLA algorithm.

the input fragility models and, when available, override those calculated with OpenQuake. This calculation flow was adopted in an attempt to accommodate the needs of an operational real-time system in which, for example, the instruments used for the continuous monitoring of the buildings' structural health may face issues when an

earthquake occurs (such as going offline or clipping).

As a last step, economic losses and human casualties are calculated using the resulting damage states of the buildings. The economic losses calculated in this way are cumulative by nature. On the contrary, as the building occupants are updated before running calculations for each earthquake, the human casualties are incremental and only due to the earthquake being processed. Cumulative human casualties and incremental economic losses are calculated by the RTLs at the end of all RLAs and OELFs for the whole sequence, if the corresponding option has been set to True in the configuration file.

For each RLA, the user can provide either a complete rupture geometry (in the form of an OpenQuake rupture model) or a series of rupture parameters that are used by the RTLs to generate the corresponding rupture under the assumption that the input parameters correspond to a simple planar rupture type. The choice can be different for different RLA earthquakes in the triggers file, and is indicated therein. Any kind of rupture type supported by OpenQuake can be used, including complex rupture geometries. This use case of indicating different choices for different RLA triggers could, for example, address the commonly encountered situation that complex finite fault rupture models may only be available for the largest event(s) in a sequence but not for other damaging aftershocks. In the aftermath of a real earthquake, the RTLs can be re-run repeatedly as new information about the earthquake source (e.g., moment tensor, finite-fault rupture) becomes available, in a manner similar to that of the USGS ShakeMap/PAGER process (i.e., a user might run initial calculations under the assumption of a simple planar rupture and re-run

them with a more complex rupture geometry later).

3.2 Operational Earthquake Loss Forecast

An OELF is an estimate of seismic damage and loss associated with a short-term (hours, weeks, months) forecast of seismicity in a region of interest, which can be carried out by means of combining such a forecast with fragility, consequence and/or vulnerability models. Seismicity forecasts have traditionally output seismicity rates on a grid (e.g., [Iervolino et al., 2015](#)), but there has been a shift in recent years towards models that output a large number (e.g., 10,000) of stochastic earthquake catalogues (or SES) for the time span of interest (e.g., [Savran et al., 2020](#)), each of which is a possible realisation of seismicity for that time span.

This so-called event-based approach has been adopted for the RTLs, which require that independent software be used to generate the seismicity forecasts that serve as input for the OELF calculation. As a consequence, the RTLs are agnostic to the methodology and assumptions used to generate the forecasts, which means, firstly, that the RTLs are generalisable, in the sense that they can be used jointly with any existing OEF system, and, most importantly, that the RTLs can be useful to facilitate the assessment of different OEF models in terms of their outputs in the damage/loss domain in a research context. A corollary to this feature is that the use of the OELF workflow is not limited to OELF itself, but can also cover longer-term event-based probabilistic seismic risk assessments, following some adaptations to consider the longer-term replacement and repair of damaged buildings, as well as what-if induced-seismicity applications, using catalogues generated by geomechanical models/simulations as input.

In practical terms, an OELF calculation operates as a series of RLA calculations one after the other, associated with projected realisations of seismicity. However, a key challenge of working with earthquakes that have not yet occurred is the definition of the associated earthquake ruptures, which are usually not output by the methods used to generate seismicity forecasts. As a consequence, the OELF calculation in the RTLs starts by reading the input file containing the seismicity forecast and building ruptures associated with each earthquake in the forecast (Figure 5), by means of a stochastic rupture generator that makes use of a user-input uniform-area seismic source model or similar zonation to sample rupture properties. If the hypocentral depth is not part of the seismicity forecast, this is the first parameter sampled from the regional properties specified in the source zonation; the rupture nodal properties are sampled once depth is available. Then, the rupture area is calculated by means of a magnitude-to-area scaling relation supported by OpenQuake and indicated by the user in the configuration file. An initial rupture is generated from these parameters and an aspect ratio sampled uniformly from a range indicated by the user. The resulting upper and lower coordinates of the rupture are then compared against the input lower and upper seismogenic depths: if the rupture exceeds any of these

limits it gets constrained to them and the length is recalculated with this new width, preserving the overall area. An OpenQuake rupture file is created for this final rupture. Earthquakes with magnitudes below a threshold magnitude or with epicentral distances from the input exposure model larger than a threshold distance are skipped in this process (both thresholds are user-defined). This eliminates the need for a refined coordination between the geographic area used to calculate the seismicity forecasts (with third-party software) and the geographic area used within the RTLs.

Once all ruptures are built, the OELF routine goes one by one through each of the stochastic event sets (SES) contained in the seismicity forecast and, within each SES, through each earthquake, as shown in Figure 5. At the beginning of each SES, the RTLs return to the current damaged exposure model, that is, the exposure model being updated with each RLA calculation (see Figure 3). This is represented in Figure 5 by the box saying “initialise OELF exposure”. This damaged exposure model is not to be confused with the projected damaged exposure model that results from running each earthquake of an OELF calculation. Each SES starts over from the RLA-damaged exposure model and updates it internally, resulting in a projected damaged exposure model that takes into account damage accumulation within the SES and only reflects the results associated with a specific forecasted realisation of seismicity that may or may not occur.

Earthquakes that are filtered out from the seismicity catalogue due to their magnitude or epicentral distance not complying with the user-defined thresholds are assumed to cause no additional damage, economic losses or casualties, and thus the damage states up to that point in time are carried on to the next earthquake.

For each earthquake, the processing is very similar to what has been described in the RLA routine, except that no external sources of damage estimation are incorporated. Moreover, economic losses are calculated at the end of each SES, as they only depend on the final damage state. Human casualties, on the other hand, are calculated for each earthquake.

While the RTLs do store outputs of damage and losses associated with each SES, the final output of the OELF calculation is the average damage and losses due to all of the SESs. Future developments of the software could include the tracking of uncertainties and outputting of the variability across SESs.

3.3 Updating of the exposure model for cumulative damage calculations

One of the central features of the RTLs is the fact that they can account for the accumulation of damage due to a series of earthquakes affecting the same building stock in quick succession. The two main requirements associated with this feature are, firstly, the capacity to account for the current damage state of the building in order to determine the additional damage caused by the next earthquake, which is done by means of state-dependent fragility models, and, secondly, the capacity to store the current damage states so as to be able to

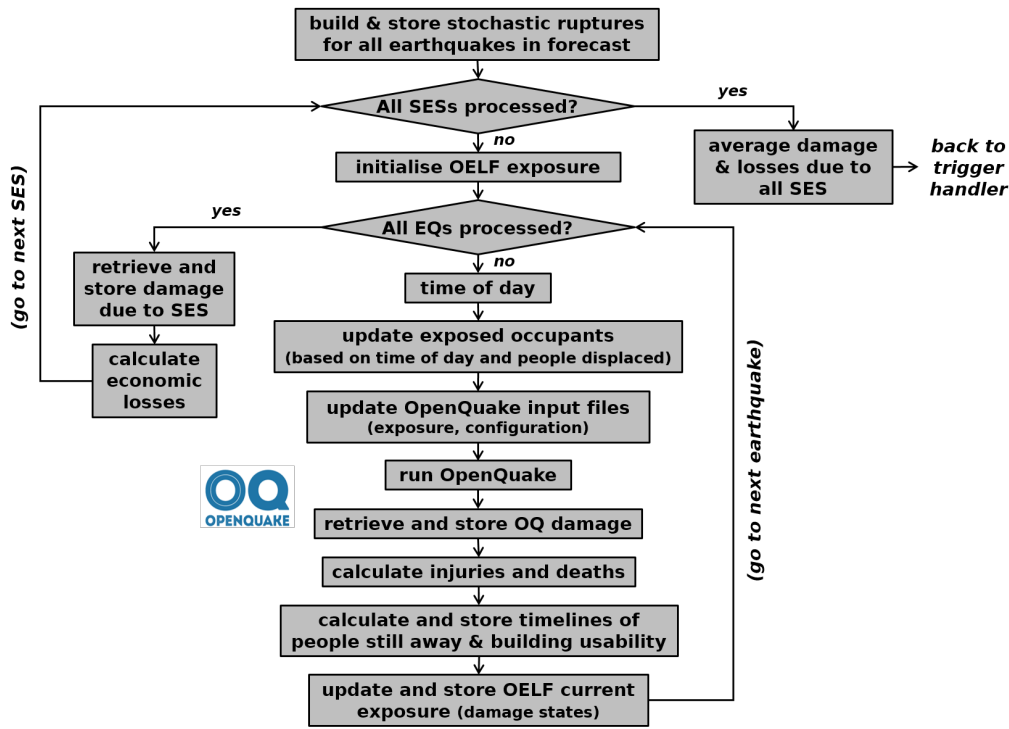


Figure 5 Main tasks of the OELF algorithm.

use them as input for said fragility models. The latter is achieved by means of updating the exposure model, which is defined in the exposure format of OpenQuake, and by appending the damage state of each asset at the end of the string that defines the building class (in the *taxonomy* column of the OpenQuake format). For example, if a standard non-RTLs damage calculation in OpenQuake uses “CLASS_A” and “CLASS_B” as building classes, the RTLs would use “CLASS_A/DS0” and “CLASS_B/DS0” to indicate an initially undamaged condition, and the same labelling would be used directly in the fragility model and/or in the file that contains the exposure-to-vulnerability conversion (these last two files as per the corresponding OpenQuake format). The naming of the damage states is user-defined.

An OpenQuake calculation that is not run through the RTLs does not require any specific aggregation of the exposure model and the user can simply define *assets*, each of which have one location and one building class and is defined by one row of the exposure file, and additional columns that can then be specified to be used for aggregation (e.g., an administrative level). While this is still possible and the RTLs make use of *assets* (i.e., each row) as well, the tools introduce two additional concepts for the exposure model: the *building_id* and the *original_asset_id*. These three concepts have a fundamental role in the calculations, as some operations are carried out at the level of the asset (with an *asset_id*), while others are carried out at the level of the *original_asset_id*. The *building_id* is intended to refer either to an individual building or an aggregation of buildings with a certain geographic meaning, while the term *original_asset_id* represents a specific building class of a specific *building_id*, in the original damage state at the beginning of the calculation. The *asset_id* then addresses different damage states of the *original_asset_id*. When the

building_id refers to an individual structure, then different *original_asset_ids* assigned to it are to be interpreted as uncertainty in the building class of that structure, and the number of buildings of all *original_asset_id* associated with one *building_id* should add up to 1. When the *building_id* refers instead to an aggregation of buildings, each *original_asset_id* is a sub-group of that aggregation that belongs to a particular building class, and the sum of the number of buildings can be any number, including non-integers (the same as in OpenQuake, as *assets* may represent expected values of an aggregated exposure model in a statistical sense and not necessarily physical buildings). In any of the two cases, damage calculations are carried out by OpenQuake for each individual *asset_id* as per the fragility curves indicated in their corresponding row of the exposure model and the exposure-to-vulnerability conversion file, and total numbers of buildings per damage state per *original_asset_id* or *building_id* are only summed up afterwards. The RTLs do not check whether a *building_id* is an individual structure or an aggregation of buildings; this distinction is purely conceptual and intended as an aid for the user to interpret the intermediate and final outputs of the RTLs.

Figure 6 illustrates the concepts of *building_id* and *original_asset_id* in three different kinds of exposure models: (a) aggregated into administrative units, (b) aggregated into 30-arcsec cells, and (c) a combination of aggregated buildings in zoom-level 18 quadtiles and individual building footprints. Different colours in the pie charts symbolise different building classes, each of which becomes an *original_asset_id* for their particular *building_id*.

The concept of *asset* of OpenQuake is maintained and referred to by the RTLs by means of an *asset_id*. In the exposure model file provided as input by the user (be-

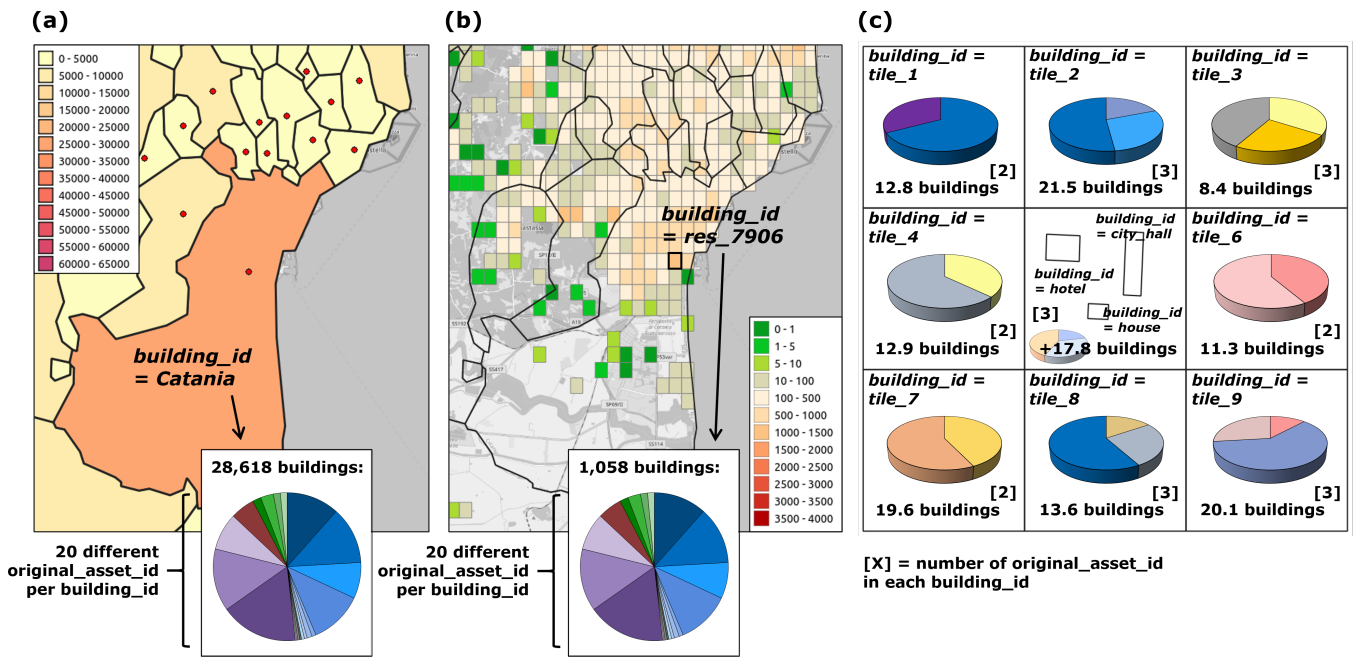


Figure 6 Illustration of the concepts of *building_id* and *original_asset_id* in three different kinds of exposure models: (a, b) ESRM20 residential exposure model (Crowley et al., 2020) for the area around Catania (Sicily, Italy) per administrative unit (a) and disaggregated onto 30-arcsec cells using the WorldPop <https://www.worldpop.org/> dataset (b). (c) Fictitious exposure model defined by Nieves et al. (2023a) following the concept of Schorlemmer et al. (2020, 2023) of combining aggregated buildings on zoom-level 18 tiles (*building_id* tile_1 through to tile_9) with individual building footprints (the three additional *building_ids* shown over the central tile) (e.g., Nieves et al., 2023b).

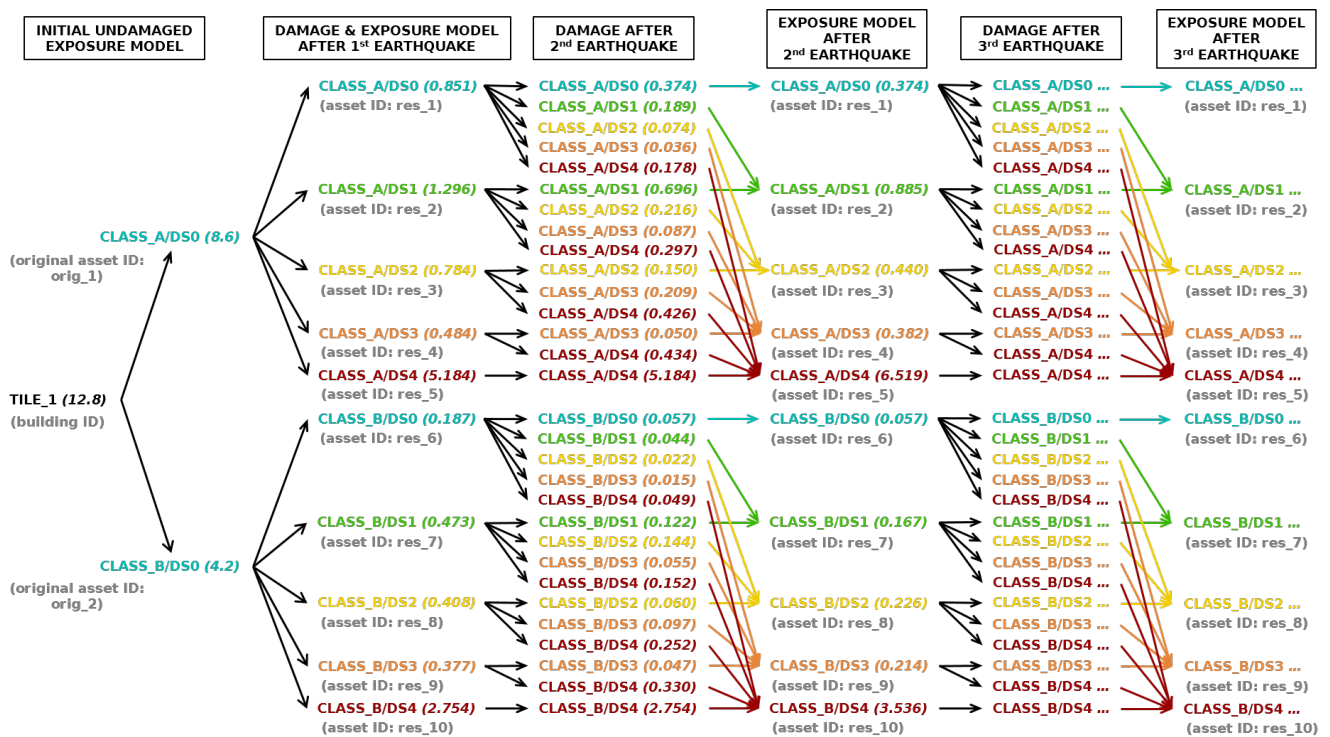


Figure 7 Schematic example of the updating of damage states in the exposure model showing one *building_id* with an aggregated building stock composed of two building classes, i.e., two *original_asset_ids*. The numbers in parentheses are the numbers of buildings.

fore the RTLs are set to run), the number of different *asset_ids* and *original_asset_ids* will be the same. However, as the calculation progresses, each *original_asset_id* will be split into as many *asset_ids* as new damage states that *original_asset_id* becomes associated with af-

ter each earthquake. As shown in Figure 7, the same damage states after an earthquake get grouped together for each *original_asset_id* for the exposure model for the next earthquake, in order to avoid an exponential increase of number of *assets* (i.e., rows in the exposure file

and, consequently, computational demand) with each earthquake. Figure 7 also shows how, by definition, assets can only remain in the same damage state or move to a worse damage state after each earthquake. This is true in the short-term, while buildings have not been repaired or replaced yet. A full scale real-time RLA/OELF system designed to run continuously should include the possibility of taking this and other longer-term changes in exposure and vulnerability into account.

Assets that reach the worst damage state (DS4 in Figure 7, for example) are not removed from the exposure model under the assumption of full destruction for two reasons. Firstly, because the damage scale is user-defined and, though logic indicates that an extreme damage state should be included, the RTLs are agnostic to the definition of the damage states. Secondly, it is much simpler from the computational point of view to keep them in the exposure model than to keep track of removed assets. This does not affect the calculations because the economic losses are always estimated based on the current damage state and thus represent cumulative losses (the economic loss associated with a destroyed building will not change because it will keep on being destroyed) and because the updating of occupants accounting for the need to inspect and repair damaged buildings takes care of not placing occupants in those buildings, as long as the user inputs reasonable average numbers of days needed for inspection and repair (those for damage states associated with complete damage or destruction should be longer than the duration of the earthquake sequence being processed).

It is not only the damage states that get updated in the exposure model after each earthquake is run. The replacement value of the building and the number of occupants are distributed proportionally to the proportions of each *original_asset_id* associated with each damage state. In the example of Figure 7, if *original_asset_id* = *orig_1* (i.e., building class “CLASS_A”) is associated with a replacement value C, then “CLASS_A/DS0” gets assigned $(0.851 / 8.6) * C$ after the first earthquake, “CLASS_A/DS1” gets assigned $(1.296 / 8.6) * C$, and so on. These replacement values get multiplied by the loss ratios of the consequence model later on, to calculate the economic losses. It is important to note that the RTLs assume that replacement values and census occupants are provided in the input exposure model for each asset, taking into account the number of buildings that conform that asset, and not in terms of a unit building of that particular building class (which is an option in OpenQuake). In the previous example, this means that the replacement value C should correspond to 8.6 buildings of “CLASS_A”. Once the replacement costs have been distributed, the economic losses are calculated using a user-input economic consequence model. The calculation of human casualties is explained in section 3.4.

Due to all this updating, the spatial extent, resolution and, more generally, the number of individual *original_asset_ids* of the exposure model play a key role in the running time of the RTLs.

It is noted that the user-defined inspection and repair times (and, consequently, the timelines of building usability) are only used by the RTLs for the purpose of

updating building occupants (to be discussed in detail in section 3.4), but not for the accumulation of damage and the calculation of the associated economic losses. Future versions of the software could expand this functionality so as to be able to effectively account for repaired buildings in all the dimensions of the calculation. Such a feature would require the additional definition of what is understood by “repair” in terms of the fragility of those buildings, that is, whether buildings should be simply taken back to their original fragility at the start of the calculation, which implies that the building is repaired to match its pre-earthquake capacity, or whether buildings would be strengthened, improved and/or replaced, which might need new building classes or definitions in the fragility model. This current limitation of the RTLs is not expected to have a large influence on results as the focus of the software (and, thus, its application to relevant case-studies) is set on the short-term, as long as the user-defined inspection and recovery times are set to be relatively long in comparison with the duration of the sequence.

3.4 Updating of building occupants

The number of occupants in buildings changes during an earthquake sequence due to a large number of factors, including deaths, injured people being taken to hospital, the need to assess the safety of structures before allowing people back in, the extreme damage of some buildings, the need to cordon off areas due to the threat posed by unstable structures to others and passers-by, interruptions to roads and/or lifelines, and so on. These are associated with the consequences of the previous earthquakes and, in the longer term, with the complex dynamics of post-earthquake recovery (e.g., Paul et al., 2024; Burton et al., 2019; Costa et al., 2022). The updating of occupants by the RTLs focuses on the first four factors listed above, which can be summarised into: (1) the damage status of the buildings and (2) the health/survival status of people. The former is represented by means of the average number of days needed to inspect and repair a building in each possible damage state (due to their own damage state, ignoring the influence that severely damaged buildings will have on the repair times of their less-damaged neighbours), while the latter is modelled by means of the average number of days associated with a hospital stay due to different degrees of injury. In this scheme, fatal injuries and instant deaths are to be represented by introducing (in the corresponding input files) a very large number of days that surpasses the duration of the earthquake sequence being run. All these are user-defined input, including the definition of the injury scale. The user is thus encouraged to use a comprehensive injury scale, so that different degrees of health status can be considered in the updating of occupants (if the scale only includes deaths, this limits the scope of the calculation).

Once occupants have been distributed across the different damage states (as explained in section 3.3), the human consequence model input by the user is used to determine the number of people suffering from each level of injury. As each level of injury is associated with

an average hospital stay, the RTLTs calculate the future point in time (in UTC) when the people with each level of injury will be able to return to their buildings as a function of their health status only, that is, irrespective of the damage status of the building. The damage status of the building is treated in a very similar way, as it is possible to calculate the future point in time (also in UTC) when the building will become usable again. All this is stored as timelines associated with each earthquake, an example of which can be seen for the application case-study in the next section (Figure 10). In the case of the health status of the occupants, the timeline describes the number of people per *original_asset_id* who are “still away” and thus need to be subtracted from the number of census occupants. In the case of the usability of buildings, the timeline stores 0 if the building is unusable or 1 if the building is usable, as a function of time. When the calculation for the next earthquake begins and thus the time of this next earthquake is known, the RTLTs go through all past timelines and retrieve the usability factors and number of people “still away” at this point in time. For each *original_asset_id*, the occupants at the time of occurrence of this new earthquake is calculated as:

$$occupants_{current} = F_{time\ of\ day} \cdot [census_{original} - still\ away] \quad (1)$$

where $F_{time\ of\ day}$ is the user-defined factor associated with the time of the day (day, night, transit time) at which the earthquake occurs, $census_{original}$ is the number of census occupants associated with the *original_asset_id*, and *still away* is the number of people unable to return to their buildings due to their health status. This number of occupants gets distributed across the different damage states (i.e., different *asset_id*) associated with the *original_asset_id* proportionally to the number of buildings in each damage state (of this *original_asset_id*):

$$occupants_{current\ DS_i} = occupants_{current} \cdot F_{occupancy\ DS_i} \cdot \frac{N_{DS_i}}{\sum_i N_{DS_i}} \quad (2)$$

where $F_{occupancy\ DS_i}$ is 0 or 1, and is retrieved from the usability timeline for damage state DS_i , $occupants_{current}$ comes from Equation 1), and N_{DS_i} is the number of buildings of *original_asset_id* in damage state DS_i .

The storage and retrieval of these future timelines of building usability and hospitalisations/deaths was preferred over the alternative of updating building occupants based on the time gap in between earthquakes input as RLA or OELF triggers, so as to resemble the needs of a potential operational real-time system in which the time of occurrence of the next earthquake would not be known *a priori*.

Carrying out these calculations at the level of the *original_asset_id*, which goes hand-in-hand with grouping assets by their new damage state as shown in Figure 7, is a simplification adopted to keep computational demand at a manageable level. In reality, each damage path (i.e., each history of moving from one damage state

to another) would have its own evolution of occupancy. Keeping track of this would mean that the logic tree presented in Figure 7 would keep on expanding after each earthquake, thus making the exposure model have more and more individual *asset_ids* at each stage and the damage and loss calculations due to the next earthquake taking longer to run.

As the user-defined inspection and repair times are not used to update the damage state of buildings (see section 3.3), the user should be cautious in their selection, to avoid the inconsistency of placing occupants back into heavily-damaged buildings that would normally not be occupied until effectively repaired (i.e., they can go back into the buildings but, for the purpose of the calculations, those buildings are still damaged). In the current version of the RTLTs, “repair” is thus better understood as the minimum action to be carried out for people to be able to use the building, though not enough to significantly set the fragility of the building back to its original state, and is the most accurate for the more superficial (i.e., non-structural) damage states.

3.5 Economic losses and human casualties

Economic losses and human casualties are calculated by means of user-defined consequence models for which an expected loss ratio is specified for each possible damage state of the fragility model. The loss ratios of the economic and human consequence models are multiplied by the replacement cost and the number of occupants in the building at the time of the earthquake, respectively, to obtain economic losses and human casualties. The current version of the RTLTs does not account for the uncertainty associated with these loss ratios, but central expected values (which are those output by the RTLTs) would not change significantly otherwise.

For each *asset_id* in a damage state DS_i , the loss is calculated as per Equation 3), where $LR_{|DS_i}$ and X_{asset_id} are the loss ratio and repair cost/number of occupants associated with *asset_id*, respectively, the latter of which results from multiplying the total repair cost/number of occupants of the corresponding *original_asset_id* by the probability of damage state DS_i .

$$L_{asset_id\ in\ DS_i} = LR_{|DS_i} \cdot X_{asset_id} = LR_{|DS_i} \cdot X_{original_asset_id} \cdot P[DS_i] \quad (3)$$

When aggregating per *original_asset_id*, the total loss results in:

$$L_{original_asset_id} = X_{original_asset_id} \cdot \sum_{i=0}^n P[DS_i] \cdot LR_{|DS_i} \quad (4)$$

As repairs are not considered for the accumulation of damage and thus the damage state of any building can only remain the same or get worse, the economic losses calculated after each earthquake are cumulative in nature. However, as occupants are updated for each earthquake, the casualties calculated are only due to that earthquake (with the influence of previous earthquakes through the effects of cumulative damage).

3.6 Output

The whole list of output files is described in the documentation of the software within its GitLab repository, and only a general overview is given in this section.

The RTLs generate output files containing the status after each earthquake (one file per earthquake) as well as one that groups together in one file the status after all earthquakes. A distinction within the latter case is whether the output refers to the building portfolio as a whole or to individual *building_ids*. The output metrics themselves correspond to number of buildings per damage state (in the case of *building_ids* that refer to aggregated number of assets) or probabilities of the building resulting in each damage state (in the case of *building_ids* that refer to individual buildings), economic losses, and human casualties, classified by injury severity level as per the user-defined injury scale. Outputs refer in all cases to expected values, that is, the average resulting from all ground motion logic tree branches and realisations of ground motion fields, as well as all SES in the case of OELF.

If the user indicates in the configuration file that they wish to store intermediate outputs, the RTLs also output the exposure model as updated after each earthquake (otherwise only the most recent “current” version is kept), the OpenQuake damage results directly in the OpenQuake format (i.e., before being used to update the exposure model), and damage results at the end of each SES of each OELF calculation (apart from the average of all SES, which is the standard output).

4 Application to the February 2023 Türkiye-Syria earthquake sequence

This section focuses on the use of the RTLs to estimate damage and losses due to the Türkiye/Syria earthquake sequence that started on 6 February 2023 with a moment magnitude M_w 7.8 earthquake at 01:17 UTC. The earthquakes caused widespread damage and losses in south-eastern Türkiye and northern Syria, though this application focuses only on the damage and losses in Türkiye. To illustrate how the RTLs could be used to rapidly assess the impact of a sequence of events such as this, a customised risk model was assembled for this case-study application, with different input components stemming from different sources, as shown in Table 1 and the sections that follow.

4.1 Earthquake ruptures

A series of RLAs was carried out for each of the 23 earthquakes in the sequence with M_w 5 and above according to the USGS National Earthquake Information Center (NEIC) (U.S. Geological Survey, 2023a), which occurred between 6 February and 10 August 2023 (inclusive). The largest magnitudes include the initial M_w 7.8 event, followed shortly by a M_w 6.7 aftershock around 10 min later, the second major M_w 7.5 event (which occurred around 9 hours after the second and is the fourth event in the sequence), and a large aftershock of M_w 6.3 that occurred 2 weeks after the beginning of the sequence. 9 contains the complete list of earthquakes.

Component	Source
Earthquake ruptures	M_w 7.8 and M_w 7.5 earthquakes: multi-segment ruptures from the USGS ShakeMap Archive. Other earthquakes: single planar ruptures estimated from focal mechanisms.
Ground motion model	New ground motion model fitted to average spectral acceleration based on Kotha et al. (2020) and Weatherill et al. (2020).
Exposure model	(Reduced) ESRM20 exposure model in its 30-arcsec version.
Fragility model	State-dependent fragility model of Iacoletti et al. (2023).
Economic consequence model	ESRM20 median economic consequence model.
Human consequence model	Ad-hoc model for injuries and deaths based on ESRM20, HAZUS (Federal Emergency Management Agency, 2003) and the LESSLOSS project (Spence, 2007).
Recovery model	Ad-hoc model.

Table 1 Components of the model used for the present case-study.

For each of the events the earthquake source is input into the RTLs as a full finite-fault rupture. In the case of the M_w 7.8 and M_w 7.5 earthquakes, the fault sources are known to be complex multi-segment ruptures spanning over 100 km in length. Here the multi-segment ruptures are defined using the two finite fault models produced by the USGS Shakesmap Archive (U.S. Geological Survey, 2023b,c). For the other events in the sequence, however, no pre-defined finite fault models were available. In these cases, the finite fault ruptures are characterised as single planar rupture surfaces whose orientation is defined using the nodal plane of the focal mechanism that aligns with the corresponding fault rupture of the two largest shocks (evaluated manually), and whose rupture area scales with magnitude according to the inter-plate scaling relation of Leonard (2014). The location of the centroid of the moment tensor is assumed to correspond to the centre of the rupture plane. The set of 23 ruptures is shown in Figure 8, and each rupture is exported into its own OpenQuake rupture model file.

4.2 Ground motions

Having deemed the state-dependent fragility models of Iacoletti et al. (2023) suitable for this application (see 4.4), it was necessary to be able to define the ground shaking in terms of average spectral acceleration (AvgSA), consistent with the definition adopted by Iacoletti et al. (2023). They define AvgSA at a given period T_0 as the geometric mean of spectral acceleration across 10 periods evenly spaced between $0.2 T_0$ and $1.5 T_0$. The ESHM20 ground motion model (GMM) for shallow crustal seismicity is developed in terms of peak ground and spectral acceleration (Kotha et al., 2020). To adapt this to AvgSA one can adopt either a direct approach, in which a GMM is fit to provide median ground motion and its standard deviation explicitly in terms of

AvgSA, or an indirect approach in which the median and standard deviation are determined for each of the required spectral acceleration from an existing GMM accounting for the spectral cross-correlation (Kohrangi et al., 2017)). Either option is possible and supported by the RTLs and OpenQuake. For the present analysis, the direct approach was preferred, and a new GMM for Europe in terms of AvgSA was calibrated using the exact same data set and regression process as that of the Kotha et al. (2020) GMM, which formed the backbone model for ESHM20. The coefficients of the model can be found in the OpenQuake implementation³. The region-to-region variability of the new GMM in terms of source stress parameter and residual attenuation was found to be consistent with that of the Kotha et al. (2020) model, which allowed us to construct the complete 15-branch GMM logic tree for shallow crustal seismicity with the direct AvgSA GMM using the regionally-adaptable “scaled backbone” approach described by Weatherill et al. (2020, 2023); Danciu et al. (2021). Comparisons of the resulting distributions of AvgSA were made using both the direct and indirect approaches and were found to be in good agreement.

When running the RTLs, a set of 1,000 ground motion fields were sampled for each of the 15 branches of the GMM logic tree, with no conditioning on real recordings. As no spatial correlation model is available for direct AvgSA, spatial correlation of ground motion residuals was not accounted for in the current simulations. Further efforts are ongoing to extend this functionality to AvgSA in future versions of the RTLs and OpenQuake.

4.3 Exposure

The ESRM20 exposure model (Crowley et al., 2020) for residential, commercial and industrial buildings, in its 30-arcsec version⁴, was used for this application. This high-resolution exposure model is defined for 9,160,363 buildings (8,365,441.2 residential, 597,894.8 commercial, 197,027.0 industrial) associated with 2,097,133 *original_asset_ids* across 308,523 cells (*building_ids*) spanning all of Türkiye. This is computationally demanding to run in the RTLs and contains a large degree of redundancy, as the majority of sites are either too far from the rupture or have too few assets to contribute to the total loss. It was therefore decided to create a reduced exposure model by retaining only the exposure at locations that contribute significantly to the losses, determined from a preliminary loss calculation based on the two largest earthquakes. The reduced exposure model is defined for 1,884,329.3 buildings (1,726,175.6 residential, 129,627.7 commercial, 28,526.0 industrial) associated with 376,100 *original_asset_ids* across 28,814 cells (*building_ids*).

The building classes in the exposure model are described as per the GEM Building Taxonomy v3.1 (Silva et al., 2022) in terms of the material and type of the lat-

eral load resisting system, the number of storeys, and the level of seismic code design and associated lateral-force design coefficient (the latter only for reinforced concrete structures). The ESRM20 exposure model for Türkiye is based on the Population and Housing Census of the year 2000, complemented with building permits for the years 2001-2017.

Reinforced concrete buildings (both cast-in-place and pre-cast) represent 60.2% of the total building stock considered, while unreinforced masonry amounts to 38.5%. Only 0.05% and 1.3% of buildings are steel or wooden structures, respectively. Reinforced concrete buildings account for around 79% of the building occupants at any time of the day, while unreinforced masonry buildings account for 17.8%-19.7%, depending of the time of the day. In terms of monetary value, the participation of reinforced concrete and unreinforced masonry in the total of the building stock is 81.5% and 17.3%, respectively.

4.4 Fragility

While the ESRM20 fragility models would be the obvious choice to be directly applicable to the ESRM20 exposure model using the ESRM20 exposure-to-vulnerability mapping, the ESRM20 fragility models are not conditioned on pre-existing levels of damage, and the state-dependent fragility models of Iacchetti et al. (2023) were used instead. These were generated based on the capacity curves of the global database of fragility and vulnerability models of the Global Earthquake Model (GEM) Foundation (Martins and Silva, 2020). Similarly to the case of the exposure, the building classes in these models are described as per the GEM Building Taxonomy v2 (Brzev et al., 2013) in terms of the material and type of the lateral load resisting system, and the number of storeys, but the ductility level is specified instead of the level of seismic code design (and associated lateral-force coefficients). As the building classes are not exactly the same as in the ESRM20 model, the ESRM20 exposure-to-vulnerability mapping was adjusted. Whenever the ESRM20 fragility class existed directly in the set of fragility models of Iacchetti et al. (2023), it was adopted; whenever it did not, expert judgement was used by analysing the available building classes (e.g., CR/LFINF(CBH)+CDL+LFC:11.0/HBET:1-3 from the exposure model maps to the CR_LFINF-CDL-10_H2 fragility class in ESRM20, which corresponds to a building designed to a low-level code with a 10% lateral force coefficient, and CR_LFINF-DUL_H2 from the Iacchetti et al. (2023) fragility models was adopted herein, which corresponds to a building with low ductility level, without any specification on the lateral force coefficient). Both the fragility models of ESRM20 and of Iacchetti et al. (2023) use the same damage scale, which is defined in terms of yield and ultimate displacements in Martins and Silva (2020): no damage (DS0), slight (DS1), moderate (DS2), extensive (DS3) and complete (DS4) damage.

³https://github.com/gem/eq-engine/blob/master/openquake/hazardlib/gsim/weatherill_2024.py

⁴https://gitlab.seismo.ethz.ch/efehr/esrm20/-/tree/main/Exposure_30arcsec

4.5 Consequence models

The ESRM20 economic consequence model, which indicates the loss ratio associated with each damage state in the scale, was used. The economic loss ratio is defined as the quotient between the cost of repairing and that of full replacement of the building. As the current version of the RTLs does not account for uncertainty in the consequence model (though it is planned to add this feature in the future), only mean expected values are considered, which are: 0 for DS0, 0.05 for DS1, 0.15 for DS2, 0.6 for DS3, and 1.0 for DS4 (Crowley et al., 2021).

For the human casualties, the HAZUS injury classification scale (Federal Emergency Management Agency, 2003) has been used. It consists of four levels of increasing severity of injury, from injuries that only require basic medical aid that can be provided in the field (level 1), all the way to instantaneous death or mortally injured (level 4). The casualty model consists of rates (quotients of number of injured or killed people to number of people in the building) for each injury severity level, building class and damage state of the building. The casualty rates adopted herein result from combining the ESRM20 fatality model (which only focuses on deaths resulting from buildings in DS4 that collapse) with the HAZUS casualty rates modified as per the LESSLOSS project (Spence, 2007) for Turkish buildings in the case of the reinforced concrete structures and for Portuguese buildings in the case of the unreinforced masonry buildings (as no rates are available from the LESSLOSS project for Turkish unreinforced masonry buildings).

As DS4 does not refer to collapse but to damage so extensive that is irreparable, the probability of collapse given the occurrence of DS4 is accounted for in the casualty rates: a 10% probability of collapse given the occurrence of DS4 was adopted for the reinforced concrete buildings, as assumed in the LESSLOSS project (Spence, 2007), while the ESRM20 probabilities of collapse have been adopted for all other structural types (0.5% for steel and wooden buildings, 2%-5% for unreinforced masonry buildings). The 10% probability of collapse given DS4 for reinforced concrete buildings is more pessimistic than the 1%-3% range of ESRM20. The calculation of the fatality rate (injury level 4) given collapse was carried out as in the ESRM20 model (and taking several of its coefficients), accounting for the likelihood that a completely damaged building collapses to the extent that it could cause loss of life, a collapse factor (as a function of the building class), the probability of entrapment given collapse, and the probability of loss of life given entrapment, while at the same time including the casualty rates associated with DS4 buildings that do not collapse, which are not included in the ESRM20 model. As the first earthquake, which is responsible for most of the damage and losses, occurred during the night time, the probability of loss of life given entrapment during the night time was adopted for the whole sequence. This may potentially lead to an overestimation of the number of deaths calculated for the M_w 7.5 earthquake, which occurred during the day time instead. The tables in 10 show the adopted casualty rates

for each combination of injury severity level and damage state. The final fatality rates (i.e., casualty rates for injury level 4) given DS4 (including collapsed and non-collapsed buildings) adopted herein for reinforced concrete buildings are 7.4% for buildings up to four storeys and 10.25% for buildings with five or more storeys (associated with the two alternative probabilities of loss of life given entrapment adopted in ESRM20, 40% and 70% in each case). These rates are more pessimistic than the final 4.6% of the LESSLOSS project for Turkish buildings, and the range of 0.38%-2% in ESRM20 for all reinforced concrete building classes (assuming a night-time earthquake). The final fatality rates given DS4 for unreinforced masonry buildings range between 0.78% and 3.34%, and are thus very similar to the ESRM20 range (assuming a night-time earthquake as well). Whether it is realistic to assume that Turkish reinforced concrete buildings have higher fatality rates given DS4 than their unreinforced masonry counterparts has not been evaluated and is outside the scope of this application case-study.

4.6 Recovery models

The adopted average number of days a person is expected to stay in hospital due to injuries of severity 1, 2 3 and 4 are zero, three, five and infinite, respectively. The extreme values (zero and infinite) stem from the definition of the injury scale itself (no hospitalisation and death, respectively), while the other two were adopted from statistics from the Organisation for Economic Cooperation and Development (OECD, 2023) for “hospital stays that require acute care” (equated to severity 3) and “hospital stays due to childbirth” (equated to severity 2, in the absence of more appropriate data⁵).

Table 2 shows the adopted number of days associated with the inspection and repair of buildings suffering from different damage states, which were defined (by expert judgement) based on the post-earthquake timelines reported by Dolce and Di Bucci (2018) and Reuland et al. (2022), as well as several considerations described in what follows. The definition of these numbers is highly uncertain, and other choices could be made. It was assumed that people occupying buildings that did not suffer any damage would continue to occupy them; such an assumption is represented by zero days needed for inspection and repair in case of DS0. The rationale behind this assumption was that, firstly, these earthquakes occurred during the winter, and the cold temperatures may have deterred people from staying out if they could observe no damage, but, most importantly, because of the large spatial footprint of this sequence and the very short time lapses between the stronger shocks. Adopting any number other than zero would lead to no occupants being considered for subsequent earthquakes in any of the buildings of the whole exposure model, but not all buildings would be exposed to the same level of shaking for all the earthquakes and it would thus be unlikely that people evacuate undamaged buildings in largely unaffected regions due to ex-

⁵The adoption of these statistical values does not imply the actual consideration of childbirth as an injury.

Damage	Inspection	Repair	Total
DS0	0	0	0
DS1	7	15	22
DS2	45	365	410
DS3	45	1095	1140
DS4	45	1095	1140 ^(*)

Table 2 Expected number of days needed for inspection and repair suffering from different damage states used for this case-study application. (*) Large number used to simulate infinity.

tensive damage occurring elsewhere (e.g., see Figure 11 in section 4.7, where it is evident there would likely be no evacuation of undamaged buildings in the areas coloured in yellow after the first earthquake).

The inspection and repair times adopted for DS2 and above mean that buildings in such damage states did not have occupants for the rest of the sequence, as the whole set of earthquakes considered herein occur within around 6 months (much shorter than 410 or 1,140 days). In reality, adopting any number of days at least one day longer than the total duration of the sequence to be run results in the same effect. This is important for the current version of the software, in which buildings are not repaired and taken back to undamaged condition after the number of days specified in the recovery model has passed, but occupants are placed back in. Buildings in DS1 start having occupants again for some of the earthquakes at the end of the sequence (see 9). This can lead to an overestimation of the number of casualties later on in the sequence. However, this overestimation will always be smaller than the alternative of not removing *any* occupants from the buildings. Buildings in DS2-DS4 do not get occupants again.

4.7 Results

Figure 9 shows the number and percentage of buildings that result in each possible damage state after the first, second, fourth and last earthquakes, considering both the complete exposure model (top row) and only the exposure cells that belong to the eleven provinces for which post-earthquake damage assessments are publicly available (Adana, Adiyaman, Diyarbakir, Elazig, Gaziantep, Hatay, Kahramanmaras, Kilis, Malatya, Osmaniye, and Sanliurfa) (bottom row). According to this model and the assumptions of the RTLs, the largest contributor to the total damage and losses is the first earthquake, followed by the fourth one. This can be expected, as these are the two strongest shocks (M_w 7.8 and 7.5) and their spatial footprint covers a large number of exposed buildings and people. Figure 9 shows as well that the incremental contribution of the individual earthquakes is most noticeable when looking only at the eleven provinces in turn, with an initial 123,230 buildings in DS4 going up to 128,612 after the second earthquake, 179,597 after the fourth and 191,783 at the end of the sequence. When considering the whole exposure model, the initial 123,672 buildings in DS4 raise up to 193,333 by the end. As can be observed, these eleven provinces account for most of the extensive damage.

Both the economic losses and the human casualties follow a similar pattern in the relative contributions of each earthquake to the total, with the first and fourth earthquakes causing the largest increments, more modest contributions from the second and eighteenth earthquakes, and almost negligible contributions from all the rest, as shown in Table 3 and Table 4. While Table 4 focuses on injuries of severity 4 (instant deaths, mortal injuries), other severities of injuries follow the same pattern. The total calculated number of human casualties in increasing order of severity were 144,638 (level 1), 67,389 (level 2), 30,329 (level 3), and 67,443 (level 4).

The contribution of each earthquake to the overall human casualties depends not only on its severity, the potential existence of previous damage and the time of the day at which it occurs, but also on the number of people injured or killed by previous earthquakes, who cannot return to their buildings for a certain period of time. Figure 10 shows the number of injured and dead people resulting from each earthquake in the sequence, who are unable to return to buildings at each point in time. The largest contribution of the first and fourth earthquake is again apparent in the plot on the left. In all cases, the curves first peak to the total sum of people resulting in injuries with severities 2, 3 and 4, and then taper to the number of deaths (severity 4).

How the accumulation of damage and losses evolves during the sequence depends not only on the fragility and consequence models or the updating of the occupants, but also on the magnitude and depth of the earthquakes and the spatial distribution of both earthquake ruptures and exposed assets. Figure 11 shows how the initial spatial pattern of losses due to the first earthquake clearly follows the trace of the first rupture and remains relatively the same after the second and third earthquakes. A sub-segment of this strip starting to the north of the province of Hatay and finishing in the province of Malatya as well as a broader area between the traces of the first and fourth ruptures appear to be where damage accumulation has its largest effect on the results. As the fault associated with the fourth earthquake ruptures (see Figure 8), the damage and losses spread north and substantially change the situation for the city of Malatya, which had been affected to a lesser extent up to this point.

Figure 12 shows how the contribution of different earthquakes to the absolute cumulative economic losses is different across the five provinces with the largest final cumulative losses (at the end of the sequence; see location in Figure 11). Hatay, at the southern end of the first rupture, is the province with both the largest final economic losses and the largest contribution from the first earthquake, but has almost no additional losses from the fourth one, which has a more apparent contribution in the case of the other four provinces. The provinces of Malatya and K. Maras are where the contribution from different earthquakes becomes more apparent (at least in the model), starting with an initial loss of 587 million EUR that increases to around 2,474 million EUR after the fourth earthquake in the case of Malatya, and going up from 1,538 to 2,161 million EUR in the case of K. Maras. The provinces of

EQ	Time after first earthquake	Absolute value (million EUR)		Percentage of final value	
		Cumulative	Incremental	Cumulative	Incremental
1	0d 00h 00m	9,708	9,708.5	71.3%	71.31%
2	0d 00h 11m	10,070	361.4	74.0%	2.65%
3	0d 00h 19m	10,118	47.8	74.3%	0.35%
4	0d 09h 7m	12,948	2,829.9	95.1%	20.79%
5	0d 14h 16m	12,967	19.8	95.2%	0.15%
6	0d 15h 26m	12,974	6.9	95.3%	0.05%
7	0d 19h 20m	12,998	23.8	95.5%	0.17%
8	1d 01h 56m	13,021	22.9	95.6%	0.17%
9	1d 05h 54m	13,033	12.3	95.7%	0.09%
10	1d 09h 1m	13,042	8.5	95.8%	0.06%
11	1d 14h 31m	13,044	2.0	95.8%	0.01%
12	1d 16h 52m	13,050	6.2	95.9%	0.05%
13	2d 06h 31m	13,056	5.6	95.9%	0.04%
14	2d 09h 54m	13,061	5.1	95.9%	0.04%
15	6d 15h 12m	13,063	2.5	96.0%	0.02%
16	10d 18h 30m	13,069	6.3	96.0%	0.05%
17	12d 18h 14m	13,071	1.2	96.0%	0.01%
18	14d 15h 47m	13,523	452.3	99.3%	3.32%
19	21d 07h 47m	13,536	13.4	99.4%	0.10%
20	25d 01h 36m	13,539	2.6	99.4%	0.02%
21	45d 08h 2m	13,546	7.1	99.5%	0.05%
22	169d 04h 27m	13,580	34.2	99.7%	0.25%
23	185d 16h 30m	13,614	34.1	100.0%	0.25%

Table 3 Expected economic losses after each earthquake in the sequence.

EQ	Time after first earthquake	Absolute value (people)		Percentage of final value	
		Cumulative	Incremental	Cumulative	Incremental
1	0d 00h 00m	58,302	58,301.9	86.4%	86.4457%
2	0d 00h 11m	58,672	370.3	87.0%	0.5490%
3	0d 00h 19m	58,706	34.1	87.0%	0.0506%
4	0d 09h 7m	66,953	8,246.5	99.3%	12.2272%
5	0d 14h 16m	66,957	4.2	99.3%	0.0063%
6	0d 15h 26m	66,961	3.9	99.3%	0.0057%
7	0d 19h 20m	66,972	11.6	99.3%	0.0172%
8	1d 01h 56m	66,984	12.0	99.3%	0.0178%
9	1d 05h 54m	66,993	8.3	99.3%	0.0124%
10	1d 09h 1m	66,997	3.9	99.3%	0.0058%
11	1d 14h 31m	66,997	0.5	99.3%	0.0008%
12	1d 16h 52m	67,000	2.5	99.3%	0.0037%
13	2d 06h 31m	67,002	1.9	99.3%	0.0029%
14	2d 09h 54m	67,003	1.4	99.3%	0.0021%
15	6d 15h 12m	67,005	1.8	99.3%	0.0027%
16	10d 18h 30m	67,007	2.5	99.4%	0.0037%
17	12d 18h 14m	67,008	0.4	99.4%	0.0006%
18	14d 15h 47m	67,383	375.3	99.9%	0.5564%
19	21d 07h 47m	67,387	3.4	99.9%	0.0051%
20	25d 01h 36m	67,388	1.7	99.9%	0.0025%
21	45d 08h 2m	67,390	2.1	99.9%	0.0031%
22	169d 04h 27m	67,431	40.3	100.0%	0.0598%
23	185d 16h 30m	67,443	12.7	100.0%	0.0188%

Table 4 Expected instant deaths and/or mortal injuries (injuries of severity 4) after each earthquake in the sequence.

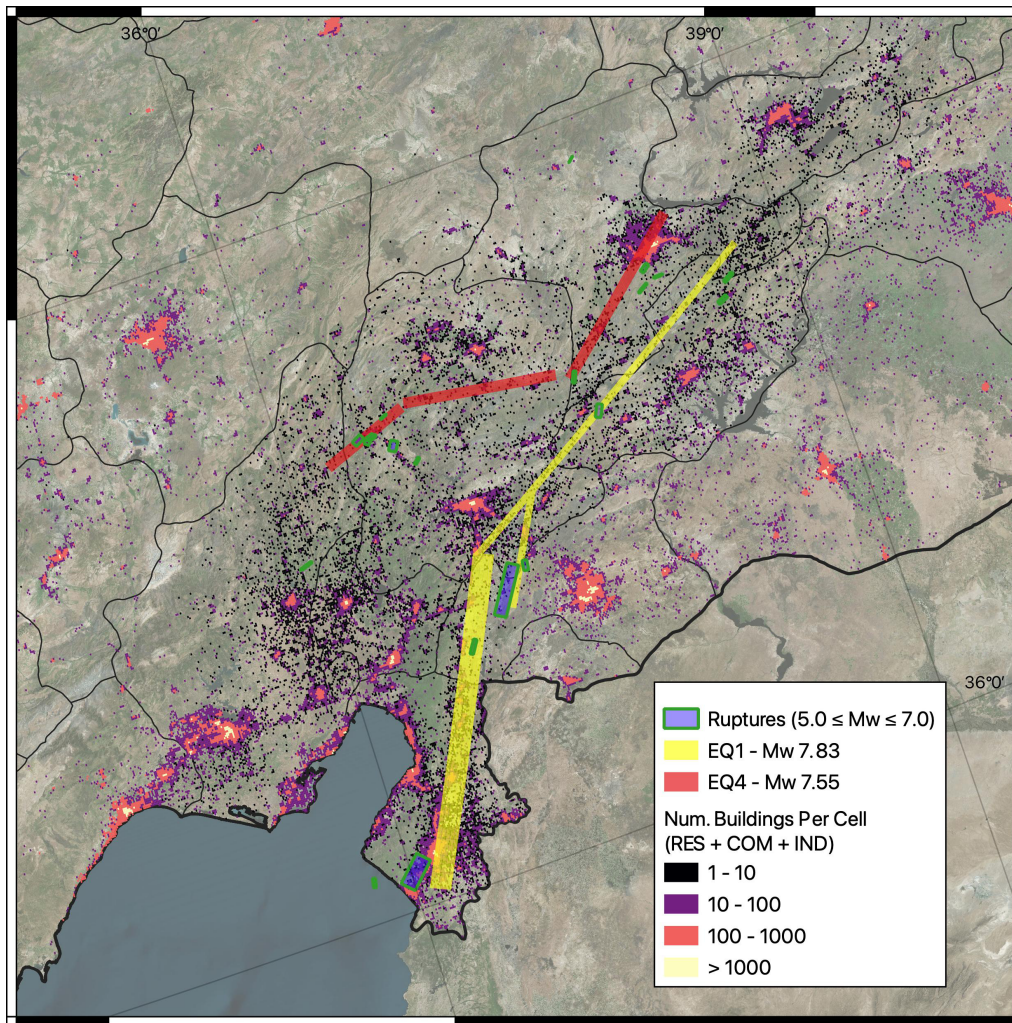


Figure 8 Location of the 23 ruptures used in the earthquake sequence, with the USGS multi-segment ruptures for the M_w 7.83 and M_w 7.55 events shown in yellow and red respectively. Cells used in the reduced version of the high-resolution exposure model are shown colour scaled according to the total number of buildings per 30 arc-second cell.

Gaziantep and Adiyaman represent somewhat intermediate cases. Figure 13 illustrates how the contribution of different earthquakes to the evolution of the cumulative losses at individual locations (in this case, 30-arcsec cells) can be variable even within the same province.

These geographic differences arise as well when comparing cumulative economic losses calculated using state-dependent fragility models (the results presented so far) against those estimated with state-independent models instead. Cumulative economic losses after the fourth earthquake calculated using state-independent fragility models⁶ independently for each earthquake (adding up the individual unconnected contributions) are larger than when using state-dependent models, but only by 0.4% for the province of Hatay, whose losses are largely dominated by the first earthquake, around 7-8% for the provinces of K. Maras, Gaziantep and Adiyaman, and up to 14% for the province of Malatya, which has a significant contribution from the first and fourth events. This is interpreted as resulting from severely damaged buildings being “damaged twice” during the first and fourth earthquakes, that is, starting to

count losses again from zero further along in the sequence when a significant part of the losses had already occurred. When using the same state-independent fragility models but progressively combining the independent probabilities of exceedance from all previous earthquakes (as explained in 8), the total losses in the province of Hatay after the fourth earthquake are almost the same as in the state-dependent case (99.85%), while those in the other four provinces are around 97-98% (i.e., 2-3% smaller). While, at first sight, these comparisons may suggest that very similar results can be obtained with any of the three approaches, a different picture emerges when looking at results at the level of the 30-arcsec cells that make up the exposure model. In the case of Hatay, cumulative economic losses after the fourth earthquake obtained adding up losses calculated using state-independent fragility models from individual earthquakes are mostly 0-15% larger in individual 30-arcsec cells than when using state-dependent models, but up to 50% larger in the case of individual cells of the provinces of Malatya, K. Maras and Gaziantep (Figure 14). When using state-independent fragility models but combining the independent probabilities of exceedance from all previous earthquakes, cumula-

⁶The state-dependent fragility models of Iacchetti et al. (2023) conditioned on no initial damage (i.e., DS0) were used for these comparisons.

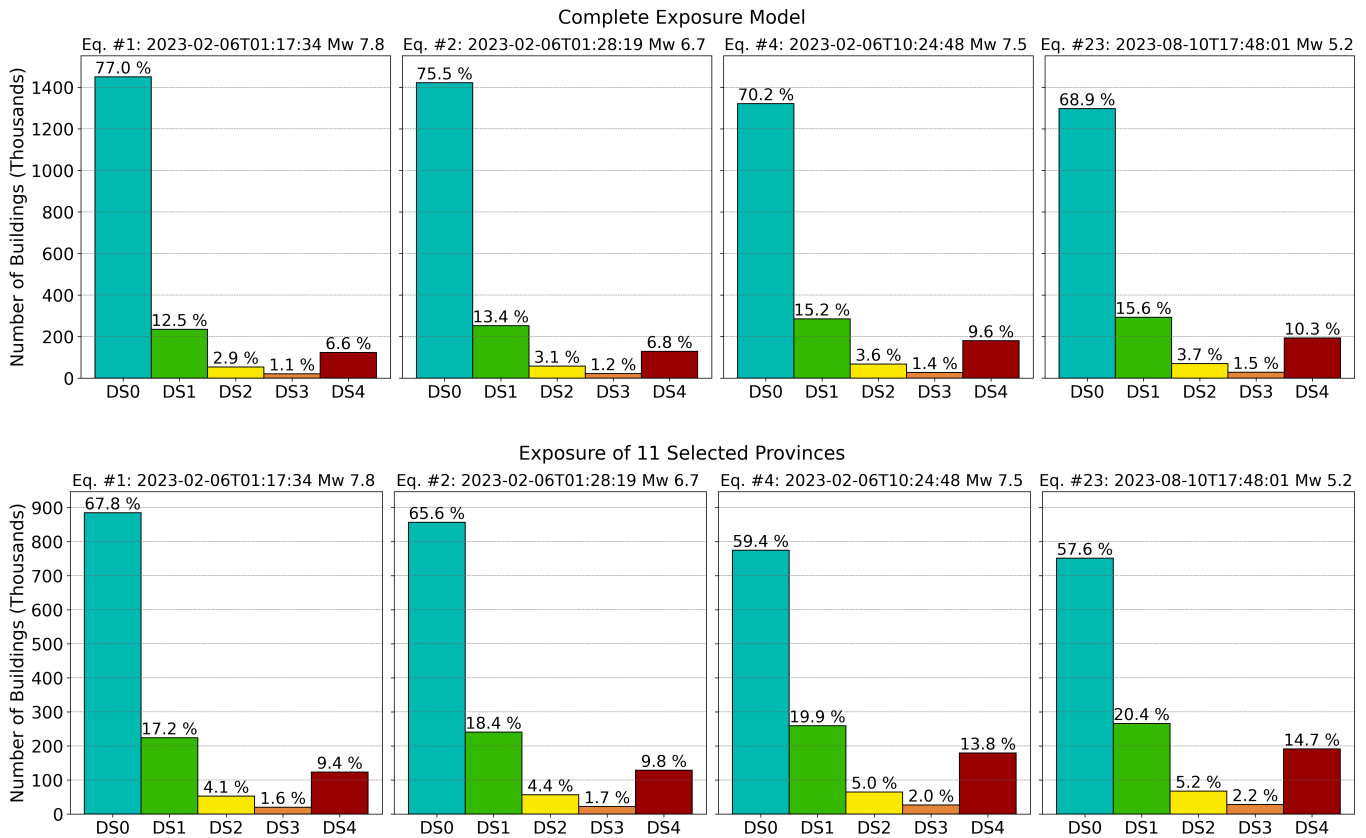


Figure 9 Expected number and proportion of buildings in each damage state after the 1st, 2nd, 4th and 23rd earthquakes for the whole exposure model (top row) and the cells corresponding to the eleven provinces for which post-earthquake damage assessments are available (bottom row).

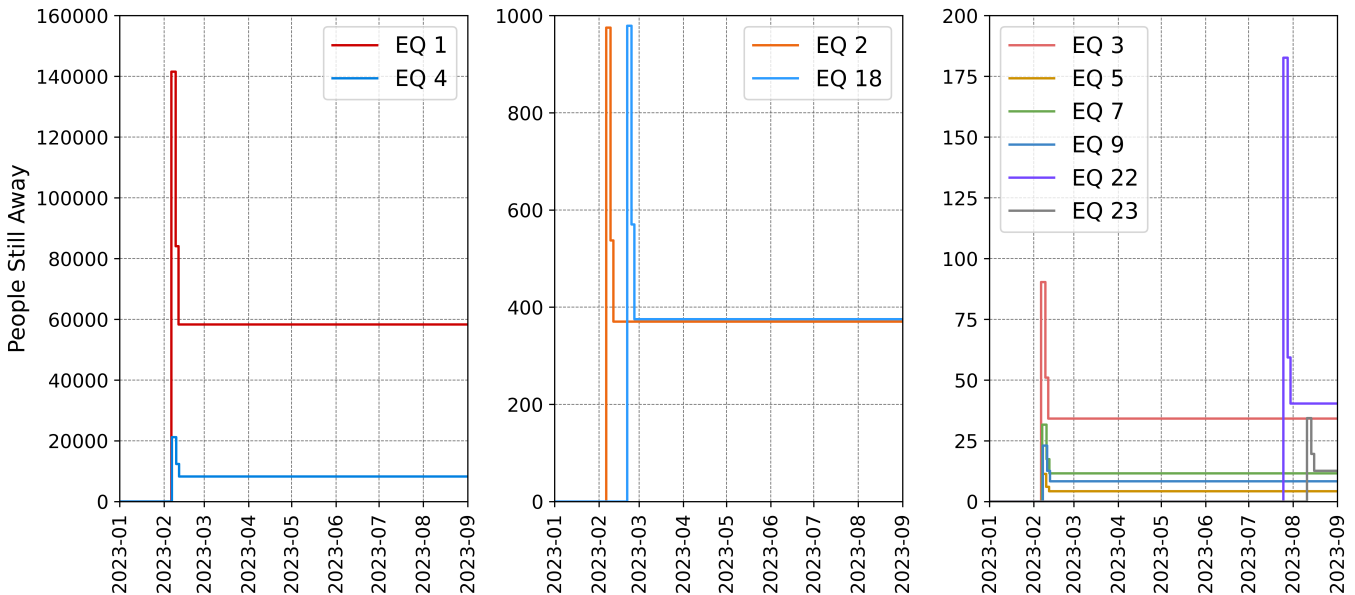


Figure 10 Number of people who are not able to return to their buildings due to their own health status at each point in time, for a selection of the 23 earthquakes of the sequence: the two largest shocks are shown on the left, the second two largest in the middle, and selected smaller events on the right (note the different vertical axes).

tive economic losses in individual 30-arcsec cells after the fourth earthquake are around 0-5% smaller than those of the state-dependent case for the provinces of Hatay, Gaziantep and Adiyaman, but up to 10% smaller for the provinces of Malatya and K. Maras (Figure15). This comparison reveals not only the relevance of prop-

erly accounting for damage accumulation for the assessment of losses at the local level, but also the risk of evaluating this relevance aggregating losses from vast areas in which local effects might average out. The resulting differences in losses calculated with different approaches cannot be generalised, as the importance

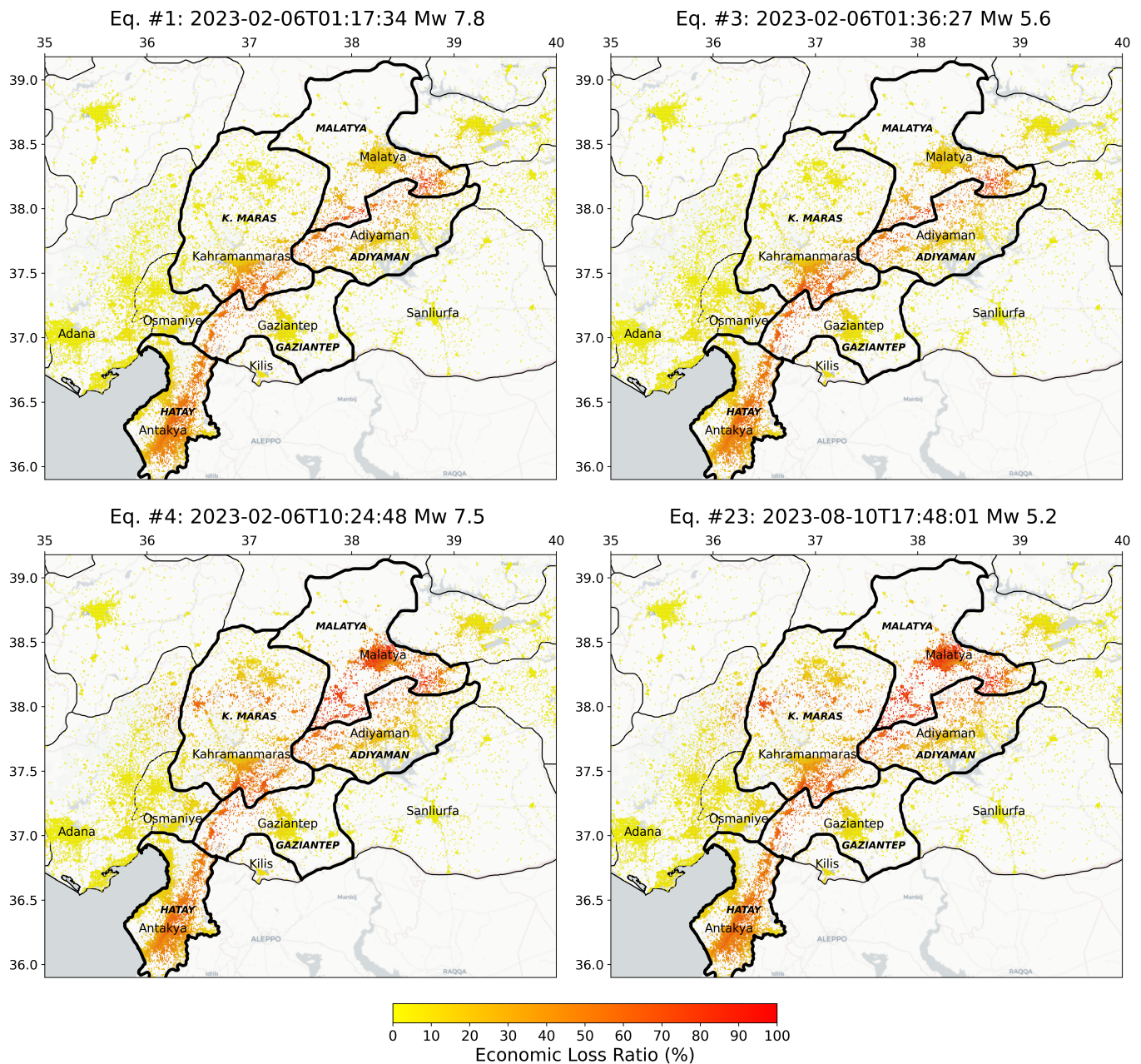


Figure 11 Evolution of the cumulative economic loss ratio per 30-arcsec cell of the exposure model after the first, third, fourth and last earthquakes of the sequence. The five provinces with the largest cumulative economic losses at the end of the sequence are marked with thicker contour lines and labelled in bold italics. Background map: Positron, Carto Basemaps (<https://carto.com/basemaps>, accessed January 2024).

of accounting for the accumulation of damage is heavily influenced by the spatial distribution of the exposed assets and their relative position with respect to the spatial distribution of the earthquakes in the sequence, as well as the relative strength of the ground motions caused by each individual earthquake (e.g., when using state-independent fragility models and adding up individual unconnected losses from each earthquake, stronger initial ground motions can lead to damage being double-counted, while weaker initial ground motions can lead to damage after further events being underestimated due to ignoring the increase in vulnerability of the building stock, which has been damaged enough to be weaker but not so much as to be completely destroyed). Examples of other spatial and tem-

poral patterns of evolution of damage can be found in Nieves et al. (2023a).

While the intent of this section is to provide an illustration of the capabilities and outputs of the RTLts to model a real seismic sequence and not to reproduce the damage and losses resulting from the 2023 Türkiye/Syria earthquake sequence or investigate the source of potential discrepancies, a sanity check was carried out by comparing the resulting number of buildings in each damage state against real post-earthquake assessment data. The data used was collected for the eleven provinces listed earlier and published by Hacettepe University Department of Civil Engineering (2023), with total numbers very close to those reported by GEER-EERI (2023) and UNDP PDNA. It is not fully

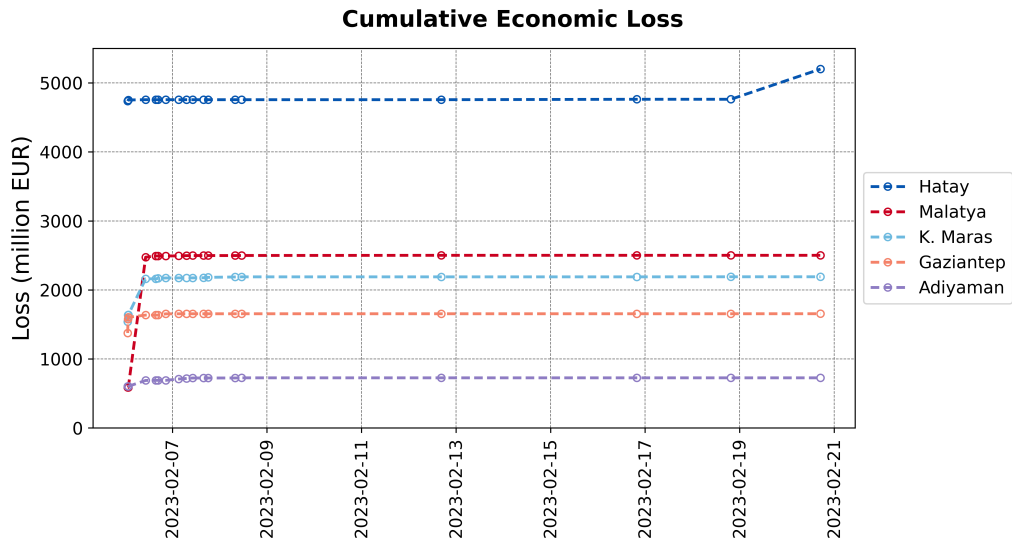


Figure 12 Evolution of absolute cumulative economic losses per province (only first 18 earthquakes shown for clarity).

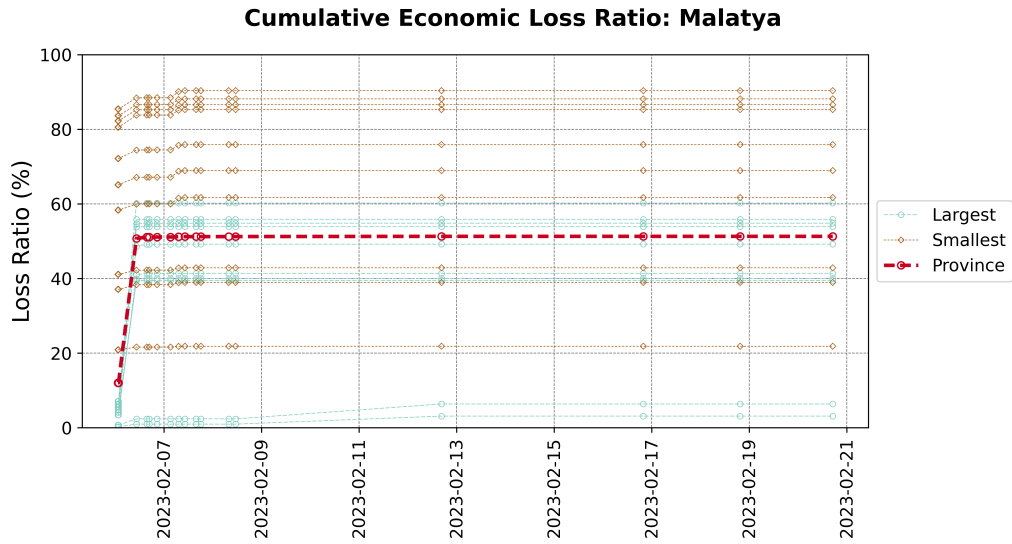


Figure 13 Evolution of cumulative economic loss ratios for the province of Malatya (red line) and for the ten 30-arcsec cells of this province with the largest (aquamarine) and smallest (brown) ratios of final loss (at the end of the sequence) to initial loss (after the first earthquake); only first 18 earthquakes shown.

clear from these sources whether the assessed buildings are only residential or a mix of different occupancy cases, though the latter appears as more likely. Four alternative conversions between the damage scale used by Hacettepe University Department of Civil Engineering (2023) and that of ESRM20 (used herein) were investigated, as shown in Table 5, with results in terms of number and proportion of buildings presented in Table 6 and Figure 16, respectively. The decision to consider different conversions stemmed, firstly, from the knowledge that thresholds between damage states and the allocation of one building to one damage state or the other by an inspector in the field have a relevant subjective component, and, secondly, from looking at what looks almost like a “swap” between numbers of buildings associated with heavy damage or collapse/urgent demolition, when considering alternative A1. Grouping these categories (as well as the two lower damage states) in alternative A2 leads to a much stronger agree-

ment. Alternatives A3 and A4 explore different ways of splitting the “heavy damage” category of Hacettepe University Department of Civil Engineering (2023) across DS4 and DS3, considering 50% of “heavy damage” corresponding to DS3 and all of “collapse/urgent demolition” plus the other 50% of “heavy damage” corresponding to DS4 in alternative A3, and considering 2/3 of “heavy damage” corresponding to DS3 and all of “collapse/urgent demolition” plus the other 1/3 of “heavy damage” corresponding to DS4 in alternative A4. As can be observed in the tables, A3 leads to a better agreement than A4. With the tuning of the model required to establish a perfect match to the observed losses out of the scope of the present work, we deem the results presented reasonable in light of the real damage observations and their uncertainties. The interested reader is referred to 11 for province-by-province comparisons.

Alternative:	A1					A2			A3					A4				
Damage state(s):	DS0	DS1	DS2	DS3	DS4	DS0+1	DS2	DS3+4	DS0	DS1	DS2	DS3	DS4	DS0	DS1	DS2	DS3	DS4
Collapse/urgent demolition	-	-	-	-	100	-	-	100	-	-	-	-	100	-	-	-	-	100
Heavy damage	-	-	-	100	-	-	-	100	-	-	-	50	50	-	-	-	66.6	33.3
Moderate damage	-	-	100	-	-	-	100	-	-	-	100	-	-	-	-	100	-	-
Light damage	-	100	-	-	-	100	-	-	-	100	-	-	-	-	100	-	-	-
No damage	100	-	-	-	-	100	-	-	100	-	-	-	-	100	-	-	-	-

Table 5 Alternative conversions (labelled A1 through A4) explored between damage scales used by Hacettepe University Department of Civil Engineering (2023) and herein (ESRM20). Values are percentages of the Hacettepe University Department of Civil Engineering (2023) scale to be compared against each of the ESRM20 damage states (e.g., according to A4, 33.3% of buildings with heavy damage plus 100% of collapsed/demolished buildings are compared against 100% of buildings estimated to be in DS4 in our calculations)

Hacettepe University damage scale	A1		A2		A3		A4	
	Hacettepe	Model	Hacettepe	Model	Hacettepe	Model	Hacettepe	Model
Collapse/urgent demolition ^(*)	53,700	191,783	238,688	220,243	146,194	191,783	115,363	191,783
Heavy damage ^(*)	184,988	28,459			92,494	28,459	123,325	28,459
Moderate damage	40,190	67,593	40,190	67,593	40,190	67,593	40,190	67,593
Light damage	419,832	266,264	1,293,924	1,018,041	419,832	266,264	419,832	266,264
No damage	874,092	751,777			874,092	751,777	874,092	751,777
Total	1,572,802	1,305,877	1,572,802	1,305,877	1,572,802	1,305,877	1,572,802	1,305,877

Table 6 Number of buildings in each damage state or damage state grouping, as per the four alternative conversions (A1 through A4) defined in Table 5. ^(*) Please note the splitting of "Collapse/urgent demolition" and "Heavy damage" varies per alternative.

The total number of deaths ranging from 58,302 at the beginning of the sequence (i.e., due only to the first earthquake) to 67,443 by the end of the sequence are larger than the 48,000 reported by UNDP PDNA as of mid-March 2023 (with the clarification that “thousands [are] still reported missing”), the 45,968 confirmed deaths in Türkiye as of 8 March 2023 reported by STEER-EERI (Dilsiz et al., 2023) and even the 50,783 deaths currently reported in Wikipedia⁷, though the order of magnitude can be deemed as good. Assuming that only injuries of severity 2 and 3 would be reported as injuries (as injuries of severity 1 do not require hospitalisation), the total of 97,718 at the end of the sequence is smaller than the “more than 100,000” and “more than 126,000” reported by STEER-EERI (Dilsiz et al., 2023) and UNDP PDNA, respectively but, as with the case of the deaths, of a good order of magnitude.

5 Concluding remarks

This paper has presented the *Real-Time Loss Tools* (RTLs), an open-source software that carries out damage and loss calculations due to earthquake sequences accounting for damage accumulation and the displacement of the building occupants along the process, as well as external sources of damage estimation. The RTLs rely on the well-established, vastly tested and also open-source OpenQuake engine (Pagani et al., 2014; Silva et al., 2013) to estimate ground motions and calculate damage due to each earthquake.

The application of the RTLs to the 2023 Türkiye/Syria earthquake sequence presented herein illustrates not only the computational capabilities of the software but also the fundamental spatial component of the dynamics of damage accumulation and the relocation of people during an earthquake sequence, in particular one whose effects span such a large geographic area. While the largest contributors to the economic losses and human casualties are the two largest shocks (M_w 7.8 and 7.5), their relative contribution varies at different locations: the losses in the province of Hatay are dominated by the first large shock (M_w 7.8), but Malatya shows a stronger contribution from the second one (M_w 7.5), while still presenting relevant losses for the first one. It is in the provinces of Malatya and K. Maras that the effect of damage accumulation becomes more visible in the present model, while appearing as almost negligible in Hatay. Economic losses calculated using state-independent fragility models independently for each earthquake and adding up the individual contributions (i.e., not accounting for damage accumulation) are 0.4% larger for the province of Hatay but 14% larger for the province of Malatya, when compared against those calculated with state-dependent fragility models (the main results presented herein). The discrepancies are even larger when looking at individual 30-arcsec cells of the exposure, and reach up to 50%. The fact that economic losses are larger when ignoring cumulative damage calculations is interpreted as a conse-

quence of starting to count losses again from zero further along in the sequence when a significant part of the losses had already occurred, though this may be different for other earthquake sequences. When using the same state-independent fragility models but progressively combining the independent probabilities of exceedance from all previous earthquakes (as explained in 8), the losses per province are around 0-3% smaller than those calculated using state-dependent fragility models, but up to 10% smaller in individual 30-arcsec cells of the provinces of Malatya and K. Maras. These comparisons highlight both the relevance of properly accounting for damage accumulation for the assessment of losses as well as taking into account the spatial extent and aggregation of the exposure and results when carrying out comparisons across methods. Observations such as these can only be made when running damage and loss calculations that can account for the evolution of the two during the earthquake sequence, which the RTLs make possible. The validation of such observations in the field is undoubtedly harder, as post-earthquake field assessments have only been carried out in Türkiye after the occurrence of all the strong shocks in the sequence.

The main features of the RTLs themselves can be summarised as follows:

- They can execute a series of RLA and/or OELF calculations (or any other type of context that satisfies the requirements of either of the two in terms of input and assumptions, such as what-if scenarios) in a chronological order specified by the user.
- They account for damage accumulation by means of state-dependent fragility models and by storing current expectations of damage within the exposure model, which is updated after each earthquake.
- They account for the relocation of building occupants during the seismic sequence and at different times of the day (both features can be turned off if desired).
- They allow the user to provide an external estimation of damage for individual buildings, if desired. For example, this can come from SHM techniques or direct observations in the field.
- The OELF calculations are carried out in an event-based fashion, taking as input sets of stochastic earthquake catalogues (SES), which have become the standard output of the newest generation of short-term seismicity forecasts, instead of seismicity rates on a grid. This event-based approach facilitates the incorporation of a myriad of considerations to damage and loss modelling, such as the spatial correlation of ground motions for any particular event, as is already done in event-based probabilistic seismic hazard/risk assessments (e.g., Crowley and Bommer, 2006; Park et al., 2007; Silva et al., 2013; Weatherill et al., 2015)
- They calculate numbers of buildings in each dam-

⁷https://en.wikipedia.org/wiki/2023_Turkey-Syria_earthquakes (last accessed: December 15, 2023).

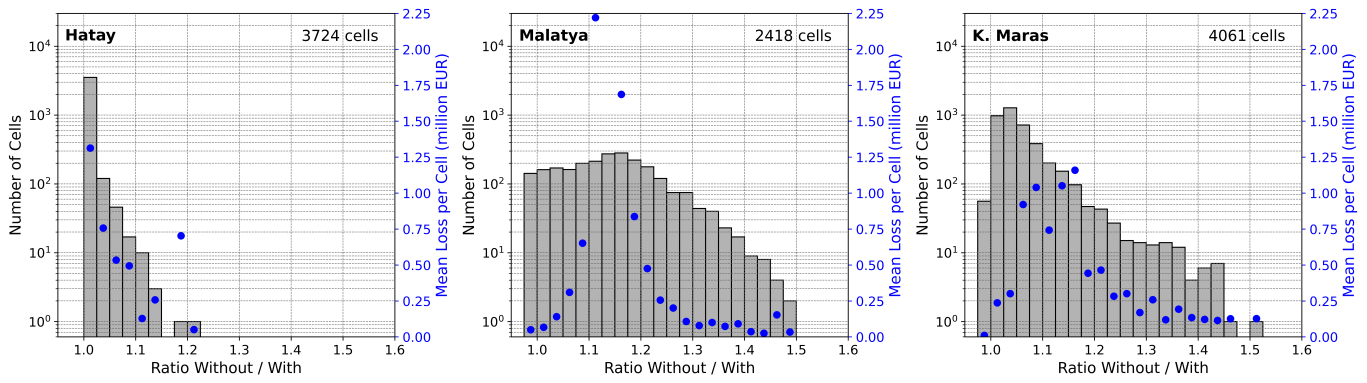


Figure 14 Ratio of cumulative absolute economic losses in individual 30-arcsec cells calculated with and without damage accumulation, the latter adding up losses calculated independently for each earthquake with state-independent fragility models, for the provinces of Hatay (left), Malatya (centre) and Kahramanmaraş (right). Mean loss per cell per bin indicated as blue dots (in millions of EUR, right-hand scale).

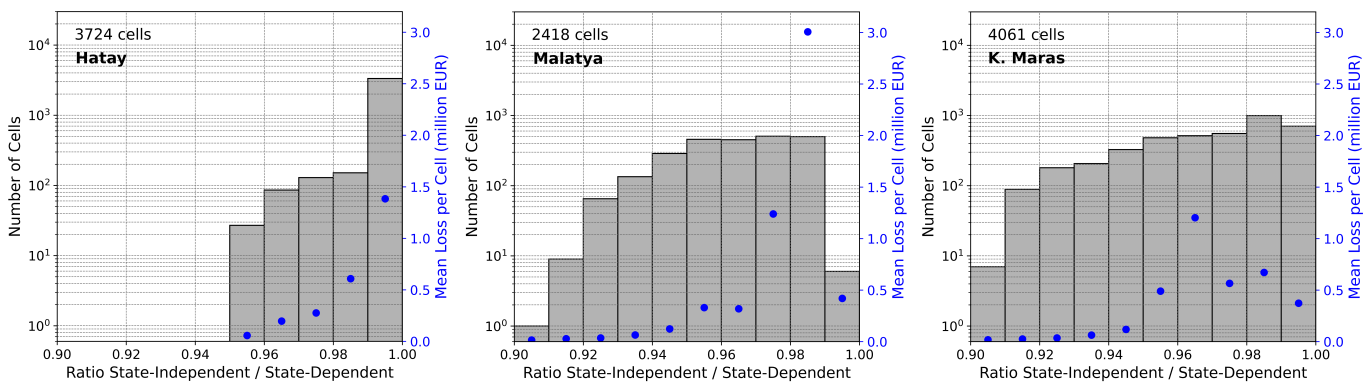


Figure 15 Ratio of cumulative absolute economic losses in individual 30-arcsec cells calculated with state-dependent and state-independent fragility models, the latter by progressively calculating the probability of not exceeding each damage state as a function of all previous earthquakes (8), for the provinces of Hatay (left), Malatya (centre) and Kahramanmaraş (right). Mean loss per cell per bin indicated as blue dots (in millions of EUR, right-hand scale).

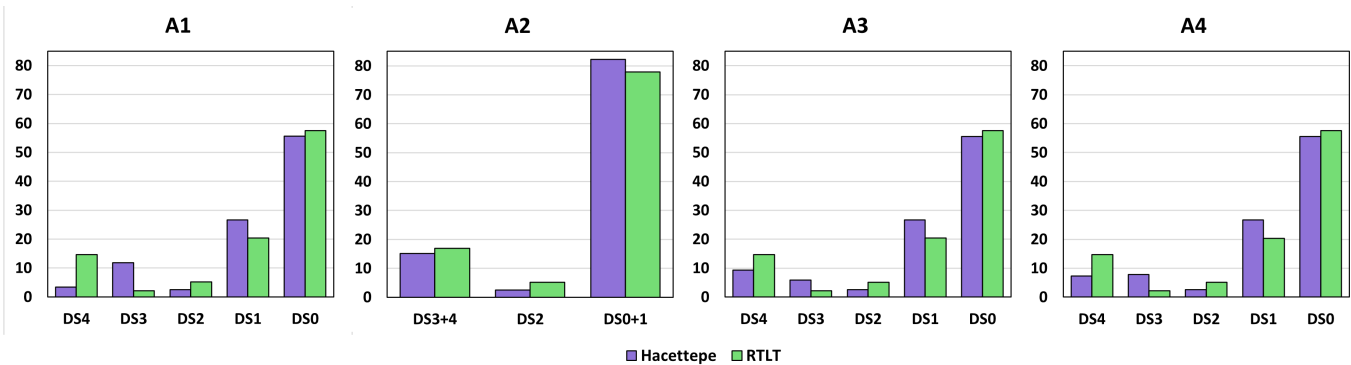


Figure 16 Proportion (%) of buildings in each damage state or damage state grouping, as per the four alternative conversions defined in Table 5.

age state, where the exposure model refers to aggregated numbers of buildings, and probabilities of a building resulting in each damage state, where the exposure model refers to individual buildings. A combination of both types of exposure is possible.

- They calculate and output economic losses and human casualties, the latter according to a user-defined injury scale.

- They can allow for damage accumulation calculations to be carried out with state-independent fragility models but progressively combining the independent probabilities of exceedance from all previous earthquakes (8). Although the accuracy of this approach has not been quantified (and likely depends on the characteristics of the earthquake sequence as well as the exposure and fragility models), this feature makes it possible to at least partly account for exposure dynamics even if state-

dependent fragility models are not yet available for the case-study under consideration.

While the connection between the RTLs and OpenQuake has only been evaluated in terms of the parameters and assumptions described herein and in the online documentation of the RTLs, any other features and capabilities of OpenQuake can be inherited as well (e.g., the conditioning of ground motion fields to recordings, the extension to secondary perils). Even if they require adaptations to the RTLs, these can be easily implemented, due to the RTLs being open-source. Planned future developments of the RTLs include the possibility of accounting for building repairs (i.e., setting back the fragility of buildings to the undamaged condition) and the incorporation and output of different kinds of modelling uncertainties, such as the variability in the economic loss ratios associated with different damage states (input consequence model) and the range of damage and losses resulting from each calculation (output).

The RTLs can be seen from different perspectives by different kinds of users. For those particularly interested in the RLA and OELF applications, the RTLs may be a starting point to develop strategies and research questions for potential future scalability and real-time operationalization in an open, transparent and customisable fashion. The exploration of the whole integration chain may facilitate the delineation of expectations for individual components and shed light on their value and the way they relate to all other components of a broader model. In this sense, the software has already been used to develop one of the final demonstration activities of the RISE project, making it possible to bring together the work and developments of different research institutions and make explicit the connections between them. Details on these demonstration activities as well as vast discussions on the requirements of a potential full-scale RLA/OELF real-time implementation can be found in [Nievas et al. \(2023a\)](#). At the same time, users interested in the capability to estimate damage and losses due to sequences of earthquakes accounting for the accumulation of damage and relocation of people due to injury/death and/or the usability of the buildings do not need to focus on whether an algorithm is labelled RLA or OELF, but on the needs and assumptions covered by each of the two routines, which can also be useful to investigate what-if cascading scenarios for decision making purposes. The application example presented in this paper illustrates the use of the RLA functionality to calculate damage/losses due to a sequence that has already occurred, rather than an ongoing sequence in real-time. Though not explored so far, the OELF functionality could potentially be used as well for longer-term probabilistic seismic risk assessments, in a similar fashion to the work of [Papadopoulos and Bazzurro \(2020\)](#). This is possible because the RTLs are agnostic to whether the input seismicity catalogues refer to short-term sequences that take place during days or months, or to a long-term seismicity model run over years, as well as to how they have been generated. For use in a long-term seismicity context, adaptations would be needed to consider the replacement and

repair of damaged buildings that can take place in such extended timeframes. In its current version, the RTLs only uses expectations of repair times to update building occupants, but not the buildings' fragilities themselves.

While the RTLs make it possible to use simple models to account for the displacement of people from their buildings due to their own health status and the need for inspection and repair of damaged buildings, data from real earthquake sequences on common recovery timelines is still relatively scarce and, in most cases, extremely dependent on governmental strategies and decisions that can be difficult to translate into a quantitative framework. For example, in the aftermath of an earthquake a government might decide that all buildings in a certain region be inspected in detail, even if they do not seem to have sustained damage at first sight, or that detailed inspections are carried out on-demand when requested by the building owners. Such a decision affects in particular the usability of buildings in the lower damage states and the undamaged condition, with the former leading to no occupants returning to any buildings for a certain period of time, and the latter leading to some buildings being re-occupied straight-away. This is one aspect within the broader scope of post-earthquake recovery, for which a model and associated plug-in for OpenQuake (OQ-RRE) were developed as part of the RISE project as well ([Reuland et al., 2022](#)), following the iRe-CoDeS framework (Interdependent Resilience Compositional Demand/Supply quantification; [Blagojević et al. \(2022\)](#); [Didier et al. \(2017\)](#)). Future work could explore ways of connecting both software, either at the coding level or in terms of making their inputs and outputs compatible.

The 2023 Türkiye-Syria case-study application presented herein illustrates the impact of the spatial distribution of seismicity, ground motions and exposed assets on the resulting damage and losses. The two extremes of a spatial distribution scale would be, on the one hand, the trivial case in which two earthquakes occur within a short period of time but so far away from each other that there is no possibility of damage accumulating and, on the other, the case in which two earthquakes occur within a short period of time so close to each other that the extent of the footprints of relevant ground shaking are almost identical. Any other case (like the one presented herein), leads to the existence of geographic areas in which more than one earthquake contribute substantially to the final damage/losses, and other areas in which most of the damage/losses are caused by only one of the events in the sequence. By taking into account the accumulation of damage during seismic sequences as an inherent part of the calculation process, the RTLs frees the user from the need to decide whether damage accumulation is to be expected in their particular case or not, and where exactly.

While the present paper has focused on a case-study application of a series of RLAs, detailed case-study applications including both RLA and OELF calculations can be found in [Nievas et al. \(2023a,d\)](#).

It is the hope of the authors that the RTLs may facilitate the application and understanding of future devel-

opments and advances on each of the components of the cumulative damage and loss calculations and that they may serve as a framework through which future innovations could eventually find their way into deployment.

Acknowledgements

This work has been developed within the Real-time earthquake risk reduction for a reSilient Europe (RISE) project, which has received funding from the European Union’s Horizon 2020 research and innovation programme under grant agreement No 821115. The authors are grateful to the RISE community for the motivating working environment and engaging discussions, and to Salvatore Iacopetti for his prompt reply to our questions on his fragility models. The authors would also like to thank, again, Salvatore Iacopetti and one anonymous reviewer for their valuable comments and suggestions, which have significantly improved the quality of this manuscript.

6 Data and code availability

The Real-Time Loss Tools are released under the GNU AGPL v3.0 license through GitLab (<https://git.gfz.de/real-time-loss-tools/real-time-loss-tools>) and Zenodo (<https://zenodo.org/doi/10.5281/zenodo.7948699>). Example input and output files can also be found on GitLab (<https://git.gfz.de/real-time-loss-tools/rise-d6-1-data-files>) and Zenodo (<https://zenodo.org/doi/10.5281/zenodo.7784841>).

The components of the European Seismic Hazard Model 2020 (ESHM20; [Danciu et al., 2021](#)) are available on GitLab: <https://gitlab.seismo.ethz.ch/efehr/eshm20>. The components of the European Seismic Risk Model 2020 (ESRM20; [Crowley et al., 2021](#)) are available on GitLab: <https://gitlab.seismo.ethz.ch/efehr/esrm20>. The fragility models of [Iacopetti et al. \(2023\)](#) are available on GitHub: https://github.com/Salvlac/sequence_frag_vuln.

7 Competing interests

The authors have no competing interests.

8 Appendix A

The state-dependent fragility models needed to properly account for damage accumulation do not always exist for all building classes that a user might be interested in. For this reason, the RTLs include the possibility to use state-independent fragility models to approximate a cumulative damage calculation, by progressively combining the independent probabilities of exceedance from all previous earthquakes. The general accuracy of this approach has not been quantified (and likely depends on the characteristics of the earthquake sequence as well as the exposure and fragility models), but it allows to avoid the potential inconsistency of losing over 100% of the value of a building when simply calculating losses independently for each earthquake

EQ	Lon	Lat	M _w	Date and Time	Depth (m)
1	37.0143	37.2256	7.8	2023-02-06 01:17:34	10.0
2	36.9470	37.1780	6.7	2023-02-06 01:28:19	10.7
3	36.6830	36.9970	5.6	2023-02-06 01:36:27	10.0
4	37.1962	38.0106	7.5	2023-02-06 10:24:48	7.4
5	38.1756	38.1900	5.4	2023-02-06 15:33:32	7.4
6	36.5078	38.0007	5.0	2023-02-06 16:43:28	10.0
7	37.0859	37.2507	5.3	2023-02-06 20:37:51	10.0
8	37.7309	37.7639	5.5	2023-02-07 03:13:12	10.0
9	38.6398	38.0971	5.4	2023-02-07 07:11:15	9.1
10	38.5700	38.0164	5.3	2023-02-07 10:18:14	13.0
11	36.4771	37.9939	5.0	2023-02-07 15:48:54	11.1
12	36.6013	37.9358	5.3	2023-02-07 18:09:59	17.9
13	36.4959	38.0061	5.0	2023-02-08 07:48:31	10.0
14	37.6611	37.9389	5.4	2023-02-08 11:11:52	9.6
15	38.0310	38.8240	5.0	2023-02-12 16:29:49	10.0
16	35.7967	36.1766	5.2	2023-02-16 19:47:49	10.0
17	36.5991	38.0696	5.0	2023-02-18 19:31:31	12.2
18	36.0251	36.1616	6.3	2023-02-20 17:04:29	16.0
19	38.2773	38.2144	5.2	2023-02-27 09:04:51	10.0
20	36.7004	37.8395	5.0	2023-03-03 02:53:43	7.1
21	36.4273	38.0109	5.3	2023-03-23 09:19:53	10.0
22	35.9502	37.5751	5.5	2023-07-25 05:44:51	11.4
23	38.2209	38.2684	5.2	2023-08-10 17:48:01	10.0

Table 7 Earthquakes of the 2023 Türkiye/Syria sequence with M_w 5 and above used in the present case-study application. Earthquake locations and time taken from the USGS National Earthquake Information Centre, except for Earthquakes No. 2 and 3 for which locations, time and magnitude are provided by the Engineering Strong Motion Database (<https://esm-db.eu/#/home>, accessed August 2023).

Injury	DS1	DS2	DS3	DS4	
				No Collapse	Collapse
Severity 1	0.05	0.2	1	10	50
Severity 2	0.005	0.02	0.5	8	15
Severity 3	0	0	0.01	4	10
Severity 4	0	0	0.01	4	ESRM20

Table 8 Indoor casualty rates (as percentage of occupants) that would be expected to reach each injury severity degree given the damage state for reinforced concrete frame and/or shear walls, including pre-cast, steel frames, wooden frames/walls buildings.

Injury	DS1	DS2	DS3	DS4	
				No Collapse	Collapse
Severity 1	0.05	0.4	2	10	50
Severity 2	0.005	0.04	0.2	2	10
Severity 3	0	0.001	0.002	0.02	2
Severity 4	0	0.001	0.002	0.02	ESRM20

Table 9 Indoor casualty rates (as percentage of occupants) that would be expected to reach each injury severity degree given the damage state for unreinforced masonry buildings.

and adding them up (i.e., restoring a building to its pristine condition mid-sequence so that it can be damaged again).

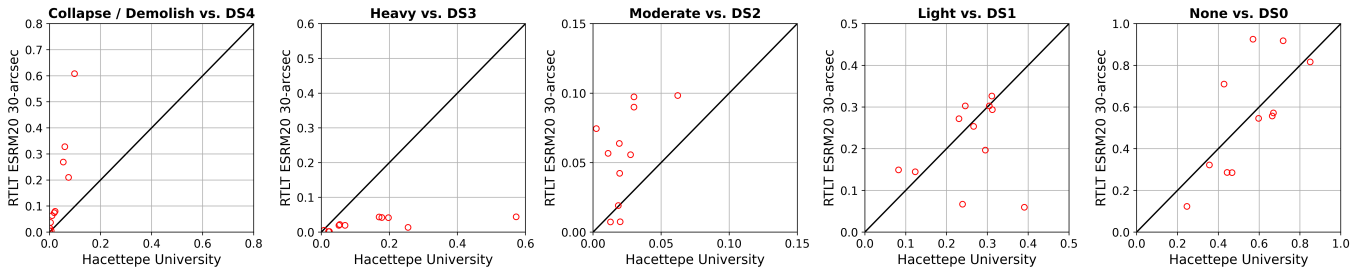


Figure 17 Proportion of buildings in each damage state using conversion alternative A1 between damage states reported by Hacettepe University Department of Civil Engineering (2023) and those calculated herein.

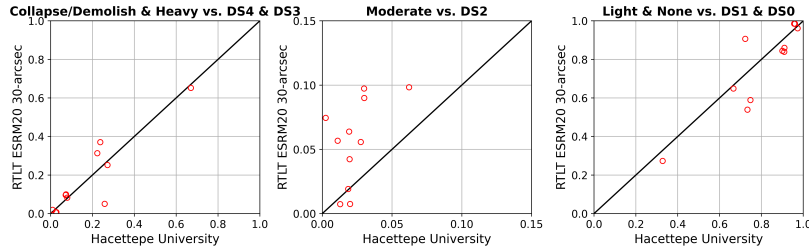


Figure 18 Proportion of buildings in each damage state using conversion alternative A2 between damage states reported by Hacettepe University Department of Civil Engineering (2023) and those calculated herein.

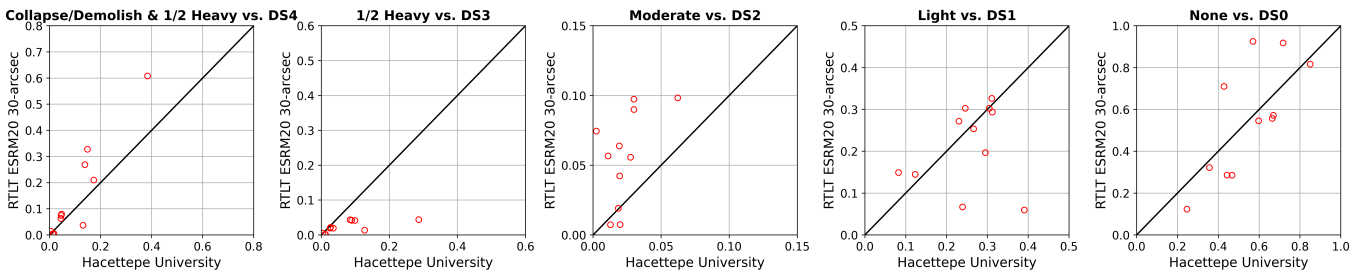


Figure 19 Proportion of buildings in each damage state using conversion alternative A3 between damage states reported by Hacettepe University Department of Civil Engineering (2023) and those calculated herein.

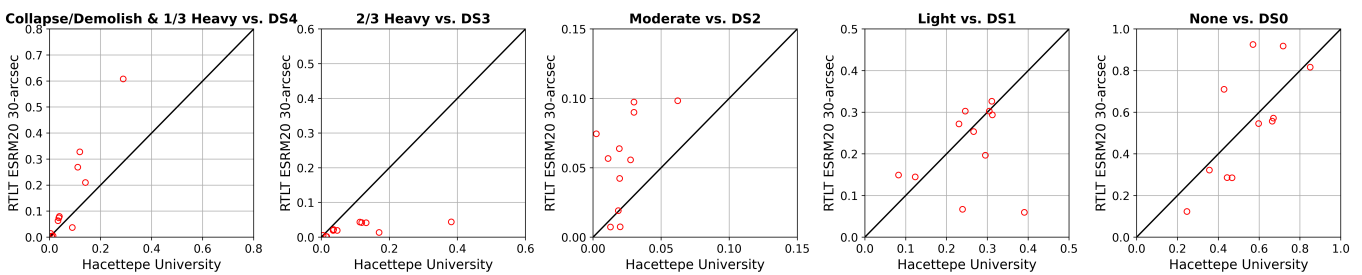


Figure 20 Proportion of buildings in each damage state using conversion alternative A4 between damage states reported by Hacettepe University Department of Civil Engineering (2023) and those calculated herein.

When using state-independent fragility models, the calculated probabilities of occurrence of each damage grade are due only to an individual earthquake m . The RTLs then work under the premise that for a damage state to not be exceeded after earthquake m it needs to not have been exceeded during any of the previous events, and for each of the previous events there is a corresponding probability. After any earthquake m in the sequence, the probability of not exceeding damage state k is calculated as per Equation 5):

$$PoNE_{cumulative_m}(DS = k) = \prod_{j=1}^m PoNE_{individual_j}(DS = k) = \prod_{j=1}^m [1 - PoE_{individual_j}(DS = k)] \tag{5}$$

where PoE and $PoNE$ are probability of exceedance and non-exceedance, respectively, *individual* refers to

the probabilities obtained from the state-independent fragility models for each individual earthquake, and *cumulative* refers to the effect of all earthquakes that have occurred up to the current one whose consequences are being calculated.

The probability of exceeding damage state k after earthquake m is simply calculated as:

$$PoE_{cumulative_m}(DS = k) = 1 - PoNE_{cumulative_m}(DS = k) \quad (6)$$

The probability of occurrence of each damage grade is then calculated as usual as the difference between probabilities of exceedance of incrementally increasing damage states. Further details can be found in the software documentation at https://git.gfz.de/real-time-loss-tools/real-time-loss-tools/-/blob/main/docs/01_Overview.md#cumulative-damage-state-dependent-vs-state-independent-fragility-models.

The inclusion of this functionality in the Real-Time Loss Tools is not to be interpreted as an encouragement or an endorsement of the approximation of cumulative damage calculations using state-independent fragility models. The use of state-dependent fragility models will always be the appropriate approach.

9 Appendix B

Table 7 summarises the hypocentral coordinates, moment magnitude and date/time of occurrence of the 23 earthquakes of the 2023 Türkiye/Syria sequence with M_w 5 and above used in the case-study application presented in section 4.

10 Appendix C

Table 8 and Table 9 summarise the casualty rates adopted in the application of the RTLs to the 2023 Türkiye-Syria earthquakes. As in HAZUS (Federal Emergency Management Agency, 2003) the fatality rates for steel and wooden buildings are almost the same as those for reinforced concrete, and no specific data for steel/wood for Türkiye was found, the reinforced concrete values were adopted for all these classes (steel and wooden buildings represent only 0.05% and 1.3% of the total number of buildings in the filtered exposure model used). The columns “Complete (collapse)” and “Complete (no collapse)” refer to DS4, for the cases in which the building classified as completely damaged collapses and does not collapse, respectively. The probability of collapse given the occurrence of DS4 was adopted as 10% for the reinforced concrete buildings, as assumed in the LESSLOSS project (Spence, 2007), and as in the ESRM20 model for all other structural types.

11 Appendix D

Figure 17 through to Figure 20 show the province-by-province (administrative level 1) comparison of proportion of buildings in each damage state as calculated herein (vertical axes) and as reported by Hacettepe University Department of Civil Engineering (2023),

using each of the four alternative conversions between damage scales defined in Table 5. The eleven provinces for which post-earthquake damage assessments are publicly available are: Adana, Adiyaman, Diyarbakir, Elazig, Gaziantep, Hatay, Kahramanmaras, Kilis, Malatya, Osmaniye, and Sanliurfa.

References

- Astorga, A. and Guéguen, P. Structural health building response induced by earthquakes: Material softening and recovery. *Engineering Reports*, 2(9):e12228, July 2020. doi: 10.1002/eng2.12228.
- Bazzurro, P., Cornell, C., Menun, C., and Motahari, M. Guidelines for seismic assessment of damaged buildings. pages 1–15. 13th World Conference on Earthquake Engineering, Aug. 2004.
- Blagojević, N., Didier, M., and Stojadinović, B. Quantifying component importance for disaster resilience of communities with interdependent civil infrastructure systems. *Reliability Engineering & System Safety*, 228:108747, Dec. 2022. doi: 10.1016/j.res.2022.108747.
- Brzev, S., Scawthorn, C., Charleson, A., Allen, L., Greene, M., Jaiswal, K., and Silva, V. GEM building taxonomy version 2.0. GEM Technical Report 2013-02 V1.0.0, GEM Foundation, Pavia, Italy, 2013.
- Burton, H., Kang, H., Miles, S., Nejat, A., and Yi, Z. A framework and case study for integrating household decision-making into post-earthquake recovery models. *International Journal of Disaster Risk Reduction*, 37:101167, July 2019. doi: 10.1016/j.ij-drr.2019.101167.
- Ceferino, L., Mitrani-Reiser, J., Kiremidjian, A., Deierlein, G., and Bambarén, C. Effective plans for hospital system response to earthquake emergencies. *Nature Communications*, 11:4325, Aug. 2020. doi: 10.1038/s41467-020-18072-w.
- Chang, S., Pasion, C., Tatebe, K., and Ahmad, R. Linking lifeline infrastructure performance and community disaster resilience: models and multi-stakeholder processes. Technical Report MCEER-08-0004, 2008.
- Chioccarelli, E., Pacifico, A., and Iervolino, I. Operational earthquake loss forecasting for Europe. RISE Project Deliverable 4.3, 2022. http://static.seismo.ethz.ch/riase/deliverables/Deliverable_4.3.pdf.
- Costa, R., Haukaas, T., and Chang, S. E. Predicting population displacements after earthquakes. *Sustainable and Resilient Infrastructure*, 7(4):253–271, 2022. doi: 10.1080/23789689.2020.1746047.
- Crowley, H. and Bommer, J. J. Modelling Seismic Hazard in Earthquake Loss Models with Spatially Distributed Exposure. *Bulletin of Earthquake Engineering*, 4(3):249–273, Apr. 2006. doi: 10.1007/s10518-006-9009-y.
- Crowley, H., Despotaki, V., Rodrigues, D., Silva, V., Toma-Danila, D., Riga, E., Karatzetzou, A., Fotopoulou, S., Zugic, Z., Sousa, L., Ozcebe, S., and Gamba, P. Exposure model for European seismic risk assessment. *Earthquake Spectra*, 36:252–273, June 2020. doi: 10.1177/8755293020919429.
- Crowley, H., Dabbeek, J., Despotaki, V., Rodrigues, D., Martins, L., Silva, V., Romão, X., Pereira, N., Weatherill, G., and Danciu, L. European Seismic Risk Model (ESRM20). EFEHR Technical Report 002, V1.0.1, 2021. doi: 10.7414/EUC-EFEHR-TR002-ESRM20.
- Danciu, L., Nandan, S., Reyes, C., Basili, R., Weatherill, G., Beauval, C., Rovida, A., Vilanova, S., Sesetyan, K., Bard, P.-Y., Cotton, F., Wiemer, S., and Giardini, D. The 2020 update of the European Seismic Hazard Model - ESHM20: Model Overview. EFEHR Tech-

- nical Report 001 v1.0.0, 2021. doi: 10.12686/A15.
- Didier, M., Broccardo, M., Esposito, S., and Stojadinovic, B. A compositional demand/supply framework to quantify the resilience of civil infrastructure systems (Re-CoDeS). *Sustainable and Resilient Infrastructure*, 3(2):86–102, Sept. 2017. doi: 10.1080/23789689.2017.1364560.
- Dilsiz, A., Gunay, S., Mosalam, K., Miranda, E., Arteta, C., Sezen, H., Fischer, E., Hakhamaneshi, M., Hassan, W., Alhawamdeh, B., Andrus, S., Archbold, J., Arslanturkoglu, S., Bektas, N., Ceferino, L., Cohen, J., Duran, B., Erazo, K., Faraone, G., Feinstein, T., Gautam, R., Gupta, A., Haj Ismail, S., Jana, A., Javadinasab Hormozabad, S., Kasalanati, A., Kenawy, M., Khalil, Z., Liou, I., Marinkovic, M., Martin, A., Merino-Peña, Y., Mivehchi, M., Moya, L., Pájaro Miranda, C., quintero, n., Rivera, J., Romão, X., Lopez Ruiz, M. C., Sorosh, S., Vargas, L., Velani, P. D., Wibowo, H., Xu, S., Yilmaz, T., Alam, M., Holtzer, G., Kijewski-Correa, T., Robertson, I., Roueche, D., and Safiey, A. StEER: 2023 Mw 7.8 Kahramanmaraş, Türkiye Earthquake Sequence Preliminary Virtual Reconnaissance Report (PVRR). Technical report, 2023. doi: 10.17603/DS2-7RY2-GV66.
- Dolce, M. and Di Bucci, D. The 2016–2017 Central Apennines Seismic Sequence: Analogies and Differences with Recent Italian Earthquakes. page 603–638. Recent Advances in Earthquake Engineering in Europe: 16th European Conference on Earthquake Engineering, Thessaloniki, Greece, 2018, Springer International Publishing, 2018. doi: 10.1007/978-3-319-75741-4_26.
- Earle, P. S., Wald, D. J., Jaiswal, K. S., Allen, T. I., Hearne, M. G., Marano, K. D., Hotovec, A. J., and Fee, J. Prompt Assessment of Global Earthquakes for Response (PAGER): A System for Rapidly Determining the Impact of Earthquakes Worldwide. U.S. Geological Survey Open-File Report, no. 2009–1131, 2009. doi: 10.3133/ofr20091131.
- Federal Emergency Management Agency. *HAZUS-MH Technical Manual*. Washington, D.C, 2003.
- GEER-EERI. February 6, 2023 Türkiye Earthquakes: Report on Geoscience and Engineering Impacts. GEER Association Report 082, 2023. doi: <https://doi.org/10.18118/G6PM34>.
- Gerstenberger, M., McVerry, G., Rhoades, D., and Stirling, M. Seismic Hazard Modeling for the Recovery of Christchurch. *Earthquake Spectra*, 30(1):17–29, Feb. 2014. doi: 10.1193/021913eqs037m.
- Guéguen, P. and Tiganescu, A. Consideration of the Effects of Air Temperature on Structural Health Monitoring through Traffic Light-Based Decision-Making Tools. *Shock and Vibration*, 2018 (1):9258675, Jan. 2018. doi: 10.1155/2018/9258675.
- Hacettepe University Department of Civil Engineering. Kahramanmaraş Pazarcık (Mw=7.7) and Kahramanmaraş Elbistan (Mw=7.6) Earthquakes Investigation Report, 2023. <https://fs.hacettepe.edu.tr/etkinlik/2023/03-Mart/rapor.pdf>. in Turkish. Last accessed December 15, 2023.
- Iacoletti, S., Cremen, G., and Galasso, C. Modeling damage accumulation during ground-motion sequences for portfolio seismic loss assessments. *Soil Dynamics and Earthquake Engineering*, 168:107821, May 2023. doi: 10.1016/j.soildyn.2023.107821.
- Iacoletti, S., Cremen, G., and Galasso, C. Investigating the sensitivity of losses to time-dependent components of seismic risk modeling. *Earthquake Spectra*, 40(2):1376–1395, Feb. 2024. doi: 10.1177/87552930231226230.
- Iervolino, I., Chioccarelli, E., Giorgio, M., Marzocchi, W., Zuccaro, G., Dolce, M., and Manfredi, G. Operational (Short-Term) Earthquake Loss Forecasting in Italy. *Bulletin of the Seismological Society of America*, 105(4):2286–2298, June 2015. doi: 10.1785/0120140344.
- Jaiswal, K. and Wald, D. Development of a semi-empirical loss model within the USGS Prompt Assessment of Global Earthquakes for Response (PAGER). Proceedings of the 9th US and 10th Canadian Conference on Earthquake Engineering: Reaching Beyond Borders, July 2010.
- Kohrangi, M., Kotha, S. R., and Bazzurro, P. Ground-motion models for average spectral acceleration in a period range: direct and indirect methods. *Bulletin of Earthquake Engineering*, 16 (1):45–65, Aug. 2017. doi: 10.1007/s10518-017-0216-5.
- Kotha, S. R., Weatherill, G., Bindi, D., and Cotton, F. A regionally-adaptable ground-motion model for shallow crustal earthquakes in Europe. *Bulletin of Earthquake Engineering*, 18(9): 4091–4125, May 2020. doi: 10.1007/s10518-020-00869-1.
- Leonard, M. Self-Consistent Earthquake Fault-Scaling Relations: Update and Extension to Stable Continental Strike-Slip Faults. *Bulletin of the Seismological Society of America*, 104(6): 2953–2965, Nov. 2014. doi: 10.1785/0120140087.
- Lilienkamp, H., Bossu, R., Cotton, F., Finazzi, F., Landès, M., Weatherill, G., and von Specht, S. Utilization of crowdsourced felt reports to distinguish high-impact from low-impact earthquakes globally within minutes of an event. *The Seismic Record*, 3(1): 29–36, Jan. 2023. doi: 10.1785/0320220039.
- Martins, L. and Silva, V. Development of a fragility and vulnerability model for global seismic risk analyses. *Bulletin of Earthquake Engineering*, 19(15):6719–6745, June 2020. doi: 10.1007/s10518-020-00885-1.
- Marzocchi, W., Lombardi, A. M., and Casarotti, E. The Establishment of an Operational Earthquake Forecasting System in Italy. *Seismological Research Letters*, 85(5):961–969, Sept. 2014. doi: 10.1785/0220130219.
- Michael, A. J., McBride, S. K., Hardebeck, J. L., Barall, M., Martinez, E., Page, M. T., van der Elst, N., Field, E. H., Milner, K. R., and Wein, A. M. Statistical Seismology and Communication of the USGS Operational Aftershock Forecasts for the 30 November 2018 Mw 7.1 Anchorage, Alaska, Earthquake. *Seismological Research Letters*, 91(1):153–173, Dec. 2019. doi: 10.1785/0220190196.
- Moon, L., Dizhur, D., Senaldi, I., Derakhshan, H., Griffith, M., Magenes, G., and Ingham, J. The Demise of the URM Building Stock in Christchurch during the 2010–2011 Canterbury Earthquake Sequence. *Earthquake Spectra*, 30(1):253–276, Feb. 2014. doi: 10.1193/022113eqs044m.
- Mouyiannou, A., Penna, A., Rota, M., Graziotti, F., and Magenes, G. Implications of cumulated seismic damage on the seismic performance of unreinforced masonry buildings. *Bulletin of the New Zealand Society for Earthquake Engineering*, 47(2):157–170, June 2014. doi: 10.5459/bnzsee.47.2.157-170.
- Nievas, C., Crowley, H., Reuland, Y., Weatherill, G., Baltzopoulos, G., Bayliss, K., Chatzi, E., Chioccarelli, E., Guéguen, P., Iervolino, I., Marzocchi, W., Naylor, M., Orlacchio, M., Pejovic, J., Popovic, N., Serafini, F., and Serdar, N. Integration of RISE Innovations in the Fields of OELF, RLA and SHM. RISE Project Deliverable 6.1, 2023a. http://static.seismo.ethz.ch/rise/deliverables/Deliverable_6.1.pdf.
- Nievas, C., Kriegerowski, M., Delattre, F., Garcia Ospina, N., Prehn, K., and Cotton, F. The European High-Resolution Exposure (EHRE) Model. Scientific Technical Report STR 23/05, GFZ German Research Centre for Geosciences, Potsdam, Germany, 2023b. doi: 10.48440/GFZ.B103-23055.
- Nievas, C. I., Crowley, H., and Weatherill, G. Real-Time Loss Tools, 2023c. doi: 10.5281/ZENODO.7948699.
- Nievas, C. I., Crowley, H. and Reuland, Y., G. Weatherill, G., Baltzopoulos, G., Bayliss, K., Chatzi, E., Chioccarelli, E., Guéguen, P., Iervolino, I., Marzocchi, W., Naylor, M., Orlacchio, M., Pejovic, J., Popovic, N., Serafini, F., and Serdar, N. Integration of RISE innovations in the fields of OELF, RLA and SHM: input and output

- datasets (Version 1.0), 2023d. doi: 10.5281/ZENODO.7784841.
- OECD. Length of hospital stay (indicator), 2023. doi: 10.1787/8dda6b7a-en. Last accessed on September 8, 2023.
- Orlacchio, M. *The effects of seismic sequences on seismic hazard and structural vulnerability*. PhD Thesis, University of Naples Federico II, Naples, Italy, 2022. http://wpage.unina.it/iuniervo/papers/Tesi_Orlacchio.pdf.
- Pagani, M., Monelli, D., Weatherill, G., Danciu, L., Crowley, H., Silva, V., Henshaw, P., Butler, L., Nastasi, M., Panzeri, L., Simionato, M., and Vigano, D. OpenQuake Engine: An Open Hazard (and Risk) Software for the Global Earthquake Model. *Seismological Research Letters*, 85(3):692–702, May 2014. doi: 10.1785/0220130087.
- Papadopoulos, A. N. and Bazzurro, P. Exploring probabilistic seismic risk assessment accounting for seismicity clustering and damage accumulation: Part II. Risk analysis. *Earthquake Spectra*, 37(1):386–408, Aug. 2020. doi: 10.1177/8755293020938816.
- Park, J., Bazzurro, P., and Baker, J. Modeling spatial correlation of ground motion intensity measures for regional seismic hazard and portfolio loss estimation. In Kanada, T. and Furuta, editors, *Applications of statistics and probability in civil engineering*. Taylor and Francis Group, London, 2007.
- Paul, N., Galasso, C., and Baker, J. Household Displacement and Return in Disasters: A Review. *Natural Hazards Review*, 25(1): 03123006, Feb. 2024. doi: 10.1061/nhrefo.nheng-1930.
- Polese, M., Di Ludovico, M., Prota, A., and Manfredi, G. Damage-dependent vulnerability curves for existing buildings. *Earthquake Engineering & Structural Dynamics*, 42(6):853–870, 2013. doi: <https://doi.org/10.1002/eqe.2249>.
- Reuland, Y., Bodenmann, L., Blagojevic, N., and Stojadinovic, B. Development of RRE forecasting services in OpenQuake. RISE Project Deliverable 4.4, 2022. http://static.seismo.ethz.ch/rise/deliverables/Deliverable_4.4.pdf.
- Reuland, Y., Martakis, P., and Chatzi, E. A Comparative Study of Damage-Sensitive Features for Rapid Data-Driven Seismic Structural Health Monitoring. *Applied Sciences*, 13(4):2708, Feb. 2023. doi: 10.3390/app13042708.
- Rossi, A., Tertulliani, A., Azzaro, R., Graziani, L., Roviada, A., Maramai, A., Pessina, V., Hailemichael, S., Buffarini, G., Bernardini, F., Camassi, R., Del Mese, S., Ercolani, E., Fodarella, A., Locati, M., Martini, G., Paciello, A., Paolini, S., Arcoraci, L., Castellano, C., Verrubbi, V., and Stucchi, M. The 2016–2017 earthquake sequence in Central Italy: macroseismic survey and damage scenario through the EMS-98 intensity assessment. *Bulletin of Earthquake Engineering*, 17(5):2407–2431, Jan. 2019. doi: 10.1007/s10518-019-00556-w.
- Savran, W. H., Werner, M. J., Marzocchi, W., Rhoades, D. A., Jackson, D. D., Milner, K., Field, E., and Michael, A. Pseudoprospective Evaluation of UCERF3-ETAS Forecasts during the 2019 Ridgecrest Sequence. *Bulletin of the Seismological Society of America*, 110(4):1799–1817, July 2020. doi: 10.1785/0120200026.
- Schorlemmer, D., Beutin, T., Cotton, F., Garcia Ospina, N., Hirata, N., Ma, K.-F., Nievas, C., Prehn, K., and Wyss, M. Global Dynamic Exposure and the OpenBuildingMap - A Big-Data and Crowd-Sourcing Approach to Exposure Modeling. Number 18920. EGU General Assembly, Copernicus GmbH, May 2020. doi: 10.5194/egusphere-egu2020-18920.
- Schorlemmer, D., Cotton, F., Delattre, F., Evaz Zadeh, T., Kriegerowski, M., Lingner, L., Oostwegel, L., Prehn, K., and Shinde, S. An open, dynamic, high-resolution dynamic exposure model for Europe. RISE Project Deliverable 2.13, 2023. http://rise-eu.org/export/sites/rise/.galleries/Deliverables/Deliverable_2.13.pdf.
- Silva, V., Crowley, H., Pagani, M., Monelli, D., and Pinho, R. Development of the OpenQuake engine, the Global Earthquake Model's open-source software for seismic risk assessment. *Natural Hazards*, 72(3):1409–1427, Mar. 2013. doi: 10.1007/s11069-013-0618-x.
- Silva, V., Brzev, S., Scawthorn, C., Yepes, C., Dabbeek, J., and Crowley, H. A Building Classification System for Multi-hazard Risk Assessment. *International Journal of Disaster Risk Science*, 13(2): 161–177, Feb. 2022. doi: 10.1007/s13753-022-00400-x.
- Sorrentino, L., Liberatore, L., Decanini, L. D., and Liberatore, D. The performance of churches in the 2012 Emilia earthquakes. *Bulletin of Earthquake Engineering*, 12(5):2299–2331, Sept. 2013. doi: 10.1007/s10518-013-9519-3.
- Spence, R. Earthquake Disaster Scenario Predictions and Loss Modelling for Urban Areas. LESSLOSS Report No.2007/07, Istituto Universitario di Studi Superiori di Pavia, 2007.
- Trevlopoulos, K., Guéguen, P., Helmstetter, A., and Cotton, F. Earthquake risk in reinforced concrete buildings during aftershock sequences based on period elongation and operational earthquake forecasting. *Structural Safety*, 84:101922, May 2020. doi: 10.1016/j.strusafe.2020.101922.
- UNDP PDNA. Türkiye Earthquakes Recovery and Reconstruction Assessment. <https://www.sbb.gov.tr/wp-content/uploads/2023/03/Turkiye-Recovery-and-Reconstruction-Assessment.pdf>. Last accessed December 15, 2023.
- U.S. Geological Survey. USGS National Earthquake Information Center, 2023a. <https://earthquake.usgs.gov>. Last accessed August 2023.
- U.S. Geological Survey. Event page for the M 7.8 - Pazarcik earthquake, Kahramanmaraş earthquake sequence, 2023b. <https://earthquake.usgs.gov/earthquakes/eventpage/us6000jllz/executive>. Last accessed February 21, 2023.
- U.S. Geological Survey. M 7.5 - Elbistan earthquake, Kahramanmaraş earthquake sequence, 2023c. <https://earthquake.usgs.gov/earthquakes/eventpage/us6000jlqa/executive>. Last accessed February 21, 2023.
- Weatherill, G., Kotha, S. R., and Cotton, F. A regionally-adaptable “scaled backbone” ground motion logic tree for shallow seismicity in Europe: application to the 2020 European seismic hazard model. *Bulletin of Earthquake Engineering*, 18(11): 5087–5117, July 2020. doi: 10.1007/s10518-020-00899-9.
- Weatherill, G., Crowley, H., Roullé, A., Tourlière, B., Lemoine, A., Gracianne, C., Kotha, S. R., and Cotton, F. Modelling site response at regional scale for the 2020 European Seismic Risk Model (ESRM20). *Bulletin of Earthquake Engineering*, 21(2): 665–714, Dec. 2023. doi: 10.1007/s10518-022-01526-5.
- Weatherill, G. A., Silva, V., Crowley, H., and Bazzurro, P. Exploring the impact of spatial correlations and uncertainties for portfolio analysis in probabilistic seismic loss estimation. *Bulletin of Earthquake Engineering*, 13(4):957–981, Jan. 2015. doi: 10.1007/s10518-015-9730-5.
- Woo, G. and Marzocchi, W. Operational Earthquake Forecasting and Decision-Making. In Wenzel, F. and Zschau, J., editors, *Early Warning for Geological Disasters: Scientific Methods and Current Practice*, page 353–367. Springer, Berlin, Heidelberg, 2014. doi: 10.1007/978-3-642-12233-0_18.
- Yeo, G. and Cornell, C. Stochastic characterization and decision bases under time-dependent aftershock risk in performance-based earthquake engineering. PEER Report 2005/13, Department of Civil and Environmental Engineering, Stanford University, Stanford, California, USA, 2005.

The article *Real-Time Loss Tools: Open-Source Software for Time- and State-Dependent Seismic Damage and Loss Cal-*

culations – Features and Application to the 2023 Türkiye-Syria Sequence © 2025 by C.I. Nievas is licensed under CC BY 4.0.